Available online at website: https://journal.bcrec.id/index.php/jcerp

Journal of Chemical Engineering Research Progress, 4 (1) 2027, 53-75

Original Research Article

Equilibrium Modeling of Dye-Antibiotic Mixture Adsorption from Simulated Pharmaceutical Wastewater onto Delonix regia Pod-Based Copolymeric Hydrogel

Ilesanmi A. Ojo[1,2,3,4*], Ayobami O. Ajani[1,2,3], Ibrahim O. Tijani[1,2,3], Akeem O. Olayiwola[2,5], Aminat A. Adetayo-Balogun[2,6], Abass O. Alade[1,2,3]

[1]Department of Chemical Engineering, Faculty of Engineering, Ladoke Akintola University of Technology, (LAUTECH), Ogbomoso, Nigeria.
[2]Bioenvironmental, Water and Engineering Research Group (BWERG), LAUTECH, Ogbomoso, Nigeria.
[3]LAUTECH SDG 6 Research Cluster (LSDGRC-6), Ladoke Akintola University of Technology, Ogbomoso, Nigeria.
[4]Department of Chemical and Geological Sciences, Faculty of Natural and Applied Sciences, Al-Hikmah University, Ilorin, Kwara State, Nigeria.
[5]Department of Pure and Applied Chemistry, Ladoke Akintola University of Technology, Ogbomoso, Nigeria.
[6]Department of Chemistry, Federal University of Agriculture and Technology, Okeho, Oyo State, Nigeria.

Received: 15th September 2026; Revised: 13th October 2026; Accepted: 26th October 2026
Available online: 16th November 2026; Published regularly: June 2027

Abstract

Many pharmaceuticals have emerged as a significant class of environmental contaminants in water bodies, posing harmful effects on natural flora and fauna. *Delonix regia* (DR) trees generate pods that accumulate as solid waste, resulting in environmental nuisances to the environment. This study aimed to utilize DR Pod (DRP) as bioresource for the development of an eco-friendly copolymeric hydrogel suitable for the remediation of Dye-Antibiotics Mixtures (DAM) in Stimulated Pharmaceutical Wastewater (SPW). DRPs sourced from the flamboyant trees at Mandate Estate, Ilorin, Kwara State, Nigeria (8.4752°N, 4.5058°E), were washed, dried, and milled. The milled DRP was used for the synthesis of the DRP Copolymeric Hydrogel (DRPCH) through free radical graft copolymerization. The DRPCH developed was characterized and used for the adsorption of DAM under batch adsorption process. Data obtained were used to determine the suitable isotherm models of DAM adsorption onto the DRPCH. The DRPCH exhibited 288% swelling capacities in water and seven hours of water retention. The moisture, ash, volatile matter, and fixed carbon content of the DRPCH were 5.90, 5.60, 25.20, and 77.95%, respectively, while its carbon, hydrogen, nitrogen, sulphur and oxygen contents were 51.80, 6.86, 2.06, 0.67, and 38.59%, respectively. The results showed that the adsorption capacity increased with increasing initial concentration. Freundlich isotherm best describes the adsorption with the Coefficient of Determination (R^2) greater than 0.95 across all the pollutants studied. This finding underscores its potential application in advanced water treatment technologies for mitigating pharmaceutical contamination in aquatic environments while simultaneously valorising the agro-residue for environmental remediation.

Copyright © 2027 by Authors, Published by Universitas Diponegoro and BCREC Publishing Group. This is an open access article under the CC BY-SA License (https://creativecommons.org/licenses/by-sa/4.0).

Keywords: Isotherms; Delonix regia Pod; Copolymeric Hydrogel; Acrlic Acid; Adsorption

How to Cite: Ojo, I. A., Ajani, A. O., Tijani, I. O., Olayiwola, A. O., Adetayo-Balogun, A. A., Alade, A. O. (2027). Equilibrium Modeling of Dye-Antibiotic Mixture Adsorption from Simulated Pharmaceutical Wastewater onto Delonix regia Pod-Based Copolymeric Hydrogel. *Journal of Chemical Engineering Research Progress*, 4 (1), 53-75. (DOI: 10.9767/jcerp.20869)

Permalink/DOI: https://doi.org/10.9767/jcerp.20869

1. Introduction

Water contamination by pharmaceutical residues and synthetic dyes has become a significant environmental concern due to their persistence, toxicity, and resistance to conventional biological treatment processes. Antibiotics such as Amoxicillin (AMO), Tetracycline (TETRA), and Ampicillin (AMP) are frequently detected in aquatic systems because a substantial fraction of administered doses is excreted unmetabolized [1]. Their continuous discharge contributes to ecological toxicity and the

* Corresponding Author.
Email: iaojo@alhikmah.edu.ng (I.A. Ojo)

development of antimicrobial resistance. Similarly, synthetic dyes used in pharmaceutical formulations and related industries possess complex aromatic structures that confer high stability and low biodegradability, thereby reducing light penetration in water bodies and disrupting aquatic ecosystems [2-4].

Dyes and antibiotics often coexist as multicomponent mixtures in real-life pharmaceutical effluents, creating competitive interactions that influence adsorption behavior. However, most adsorption studies reported in the literature focus on single-solute systems, which do not adequately represent practical wastewater conditions [5-8]. Understanding adsorption equilibrium in multicomponent systems is therefore essential for predicting adsorbent performance and optimizing treatment design [9,10].

Adsorption remains one of the most effective and economically viable techniques for removing emerging contaminants from aqueous media due to its operational simplicity and high removal efficiency at low concentrations [11]. The equilibrium relationship between adsorbate concentration in solution and the amount adsorbed at the solid surface is commonly described using adsorption isotherm models such as Langmuir, Freundlich, Temkin, Dubinin-Radushkevich, Jovanovic, and Harkin-Jura. These models provide insight into surface homogeneity, adsorption capacity, and interaction mechanisms, thereby serving as critical tools for evaluating the feasibility of newly developed adsorbent materials.

Recently, increasing attention has been directed toward low-cost adsorbents derived from agricultural wastes as sustainable alternatives to commercial activated carbon [12-16]. In tropical regions, pods of *Delonix regia* are generated in large quantities and often disposed of as solid waste. Valorization of this biomass into functional adsorbent materials offers environmental and economic advantages [9,17,18]. Novel copolymeric hydrogel synthesized from such agro-residues possesses three-dimensional polymeric networks capable of enhanced swelling and improved adsorption performance due to abundant functional groups and tunable surface properties.

Despite the growing interest in hydrogel-based adsorbents, limited studies have systematically evaluated the equilibrium behavior of multicomponent dye-antibiotic systems using biomass-derived copolymeric hydrogels. Comprehensive isotherm modeling is essential to elucidate adsorption capacity, surface characteristics, and interaction patterns in competitive systems [6]. Therefore, this study investigates the adsorption equilibrium behavior of a copolymeric hydrogel synthesized from DRP for the removal of a selected DAM from SPW under batch conditions. Experimental data were analyzed using established adsorption isotherm models to determine the best-fitting model and to evaluate the adsorption capacity and mechanism of the developed hydrogel.

2. Materials and Methods

2.1. Materials

Pods of matured *Delonix regia* were used as the precursor material for the synthesis of the copolymeric hydrogel. Acrylic Acid (AA) (LG Chem, 99.5%), Acrylamide (AM) (AM Crystal, 98.0%), N,N′-methylenebisacrylamide (MBA) (Sigma-Aldrich / Merck, 99.0%), and ammonium persulfate (APS) (Supelco / Sigma-Aldrich, 98,5%) were used as the monomers, cross-linker, and free-radical initiator, respectively. The adsorbates investigated included three antibiotics: amoxicillin, tetracycline, and ampicillin; and three dyes: Tartrazine (TARTRA) (Vidhi Dyestuffs Mfg. Ltd., 85.0%), Erythrosine (ERY) (Jagson Colorchem, 87%), and Brilliant Blue (BRIL) (Ataman Chemical, 87.0%). Ethanol (Pon Pure Chemical, 95%) and Sodium Hydroxide (NaOH) (Qualigens Q27815, 97.0%) were used during the hydrogel purification and treatment processes, respectively. All chemicals were of analytical grade and used as received without further purification.

The UV-Visible absorbance measurements were performed using a UV-Visible spectrophotometer (Genesys 150, Thermo Scientific, USA). Other equipment employed included an analytical balance (WT3003CH), orbital shaker (IKA, HS/KS 260 control), centrifuge (Scichem Tech), pH meter (Helmreasin, PHS-25), drying oven (Lemfield Medical England, DHG-9101), and muffle furnace (England Labscience, SX-4-10). Standard laboratory glassware was used for sample preparation and experimental procedures.

2.2. Preparation of *Delonix regia* Pod Powder

Mature *Delonix regia* pods were collected in Ilorin, Kwara State, Nigeria (8.4752°N, 4.5058°E). The pods were manually de-seeded, thoroughly washed with distilled water to remove adhering impurities, and sun-dried to constant weight. The dried pods were subsequently milled and sieved to obtain particles with sizes ranging from 0.11 to 0.25 mm. The resulting pod powder was stored in airtight containers until further use [18].

2.3. Synthesis of *Delonix regia* Pod Copolymeric Hydrogel

The DRP-based copolymeric hydrogel was synthesized through free-radical graft

Copyright © 2027, ISSN: 3032-7059

copolymerization, using the procedure reported by Mondal and Haque [19], with modifications to the precursor composition and reaction conditions as described below. *Delonix regia* pod powder (1.0 g) was dispersed in 20 mL of distilled water in a three-necked reaction flask equipped with a reflux condenser, nitrogen inlet, and mechanical stirring arrangement. The reaction mixture was purged with nitrogen gas for 30 min at 50 °C to minimize dissolved oxygen and establish an inert reaction environment [20-22]. Following nitrogen purging, 0.1 g of APS was added to initiate free-radical formation. Subsequently, 1.0 g of AA and 1.0 g of AM were introduced into the reaction mixture, followed by the addition of 0.25 g of MBA as the cross-linking agent. The polymerization reaction was maintained at 50 °C for 60 min under continuous stirring.

The resulting DRPCH was washed thoroughly with distilled water after polymerization, to remove residual unreacted monomers and soluble impurities. It was subsequently washed with ethanol and treated with 1.0 M NaOH solution to facilitate purification and treatment of the hydrogel network. The hydrogel was then rinsed thoroughly with distilled water and dried in an oven at 60 °C to constant mass [20,23,24]. The dried DRPCH was crushed into smaller particles and stored in airtight containers for subsequent characterization and adsorption experiments.

2.4. Characterization of DRPCH

Comprehensive characterizations, such as water absorbency, water retention time, proximate composition, and CHONS elemental analysis, were performed on the synthesized DRPCH. These are discussed in detail in subsections 2.4.1-2.4.4.

2.4.1. Water absorbency (Equilibrium swelling ratio)

Water absorbency was determined gravimetrically. Dried DRPCH (1.0 g) was immersed in 1 L of distilled water at room temperature for 24 h. After equilibrium swelling, excess surface water was removed by blotting, and the swollen sample was weighed. The equilibrium swelling ratio (Q) was calculated as Equation 1 [20,23].

$$Q = \frac{W_{final} - W_{initial}}{W_{initial}} \quad (1)$$

where $W_{initial}$ and W_{final} represent the dry and swollen weights, respectively.

2.4.2. Water retention capacity

The water retention time of the DRPCH sample at constant temperature was evaluated according to the method suggested by Zhu *et al.* [20]. Pre-equilibrated swollen sample (w_{eq}) was placed in an oven at 80 °C. The weight was recorded at 1 h intervals and recorded as w_t. Water retention percentage (w_R%) was calculated according to Equation 2.

$$W_R\,\% = \frac{w_t - w_d}{w_{eq} - w_d} \quad (2)$$

where w_t is the weight at time t, w_d is dry weight, and w_{eq} is the equilibrium swollen weight of the DRPCH sample.

2.4.3. Proximate analysis of the DRPCH developed

Proximate analysis was performed to determine moisture content, ash content, volatile matter, and fixed carbon [25]. The proximate analysis of the DRPCH developed in this study was performed based on the listed physicochemical properties in subsections 2.4.3.1-2.4.3.4.

2.4.3.1 Moisture content determination

The DRPCH sample (5 g) was placed in a pre-weighed sample container and heated in an oven at 105 °C for 24 h. The sample was transferred to a desiccator and reweighed. The moisture content removed was calculated using Equation 3 [25].

$$\text{Moisture content} = \frac{\text{Mi} - Mf}{Mi} * 100\% \quad (3)$$

where, m_i = initial mass of DRPCH and m_f = final mass of the dried DRPCH.

2.4.3.2. Determination of ash content

The DRPCH sample (2.5 g) was placed into the pre-weighed porcelain crucible and heated in a muffle furnace at 760 °C for 1 h 30 min. The crucible was cooled and subsequently reweighed. The ash content was calculated using Equation 4 [26].

$$\%\,\text{Ash} = \frac{Residual\ mass}{Initial\ mass} * 100\% \quad (4)$$

2.4.3.3. Determination of volatile matter

Volatile matter was determined by placing 1.5 g of the DRPCH sample in a silica crucible, heated at 925 °C for 7 min in a furnace. The initial weight of the crucible and DRPCH sample was recorded as w_1. The crucible was cooled in a desiccator and reweighed as w_2. The difference

Copyright © 2027, ISSN: 3032-7059

between w_1 and w_2 represents the apparent volatile matter in the sample. The actual volatile matter content was then obtained by subtracting the moisture content and expressed as a percentage of the sample [18].

2.4.3.4. Determination of fixed carbon

The fixed carbon (FC) content of the DRPCH sample was calculated by subtracting the sum of the percentages of moisture, volatile matter, and ash obtained from 100, as described in Equation 5 [25].

$$FC = 100 - (moisture\% + ash\% + volatile\ matter\%) \quad (5)$$

2.4.4. Elemental analysis of the DRPCH developed

Elemental composition (CHNOS) was determined using standard analytical procedures. Carbon content was determined via dichromate oxidation and titration as described by Ding *et al.* [27]. Nitrogen was determined using the Kjeldahl method. Sulfur content was measured spectrophotometrically at 420 nm after $BaCl_2$ complex formation. Hydrogen was determined by combustion and gravimetric water absorption. The percentage of oxygen in the DRPCH sample was obtained indirectly by deducing the difference between the total percentage of ash, carbon, nitrogen and hydrogen together and 100% as shown in Equation 6.

$$\%\,Oxygen = [100 - (\%\,Ash + \%\,C + \%\,N + \%\,H)] \quad (6)$$

2.5. Development of Dye-Antibiotics Mixture

Stock solutions of amoxicillin (287 nm), tetracycline (361 nm), ampicillin (288 nm), tartrazine (430 nm), erythrosine (500 nm), and brilliant blue (628 nm) were prepared separately. A multicomponent DAM of total concentration 100 mg/L was prepared using the I-Optimal Coordinate Exchange Design (IOCEDM) in Design Expert (13.0.1). And subsequently diluted to concentrations of 20-100 mg/L. Calibration curves were plotted for each component using the Beer-Lambert law [28,29].

2.6. Determination of Adsorbate Concentrations and Batch Adsorption

The initial concentration (Co) and equilibrium concentration (Ce) of each adsorbate were determined using a UV-Visible spectrophotometer. Calibration curves were first prepared for each adsorbate using standard solutions of known concentrations. The absorbance of each standard solution was measured at the corresponding maximum absorption wavelength of the adsorbate. A calibration curve was obtained by plotting absorbance against concentration, and the resulting linear regression equation was used to determine the concentrations of the experimental samples. The Co was determined from the concentration of the adsorbate solution before contact with DRPCH, while the Ce was determined by measuring the absorbance of the liquid phase after the adsorption experiment.

Batch adsorption experiments were conducted at room temperature to determine the effects of contact time and adsorbate concentration on the adsorption properties of the DRPCH. Samples (100 mL) of DAM solution of known initial concentration (20-100 mg/L) were mixed with 1.0 g of DRPCH in a 250 mL flask and agitated at 180 rpm. The contact time was varied between 10 and 240 min [28]. After centrifugation, the absorbances of AMO, TETRA, AMP, TARTRA, ERY, and BRI were determined at 287, 361, 288, 430, 500, and 628 nm, respectively, using a UV-Vis spectrophotometer. The adsorption capacity and percentage removal of the adsorbates were calculated using Equations 7 and 8 [14,26,30,31].

$$q_e = \frac{V\,(Co - Ce)}{m} \quad (7)$$

$$R_e = \frac{(Co - Ce)}{Co} * 100\% \quad (8)$$

2.7. Adsorption Isotherm Modeling

The adsorption equilibrium data obtained were fitted to various isotherm models, and their corresponding constants were evaluated. The selected adsorption isotherms include Langmuir, Freundlich, Temkin, Dubinin-Radushkevich, Jovanovic, and Harkin-Jura isotherms. Model suitability was evluated using Coefficients of Determination (R^2).

2.7.1. Langmuir isotherm

Six different linear forms of the Langmuir isotherm were examined to identify the model that best fits the experimental data with the least error. The Langmuir constants, b and q_{max}, were determined from the slope and intercept of the corresponding linear plots derived from Equations 9-14 [32].

$$\frac{1}{q_e} = \frac{1}{bq_{max}} \cdot \frac{1}{C_e} + \frac{1}{q_{max}} \quad (9)$$

$$\frac{1}{C_e} = bq_{max} \cdot \frac{1}{q_e} - b \quad (10)$$

$$q_e = q_{max} - \frac{1}{b}\,\frac{q_e}{C_e} \quad (11)$$

$$\frac{q_e}{C_e} = bq_{max} - bq_e \quad (12)$$

$$c_e = q_{max}\,\frac{C_e}{q_e} + \frac{1}{b} \quad (13)$$

$$\frac{C_e}{q_e} = C_e \cdot \frac{1}{q_{max}} + \frac{1}{q_{max}b} \quad (14)$$

Copyright © 2027, ISSN: 3032-7059

where q_e is the amount of adsorbate adsorbed at equilibrium (mg/g), q_{max} is the maximum adsorption capacity (mg/g), b is the Langmuir equilibrium constant (L/mg), and C_e is the equilibrium concentration of the DAM solution (mg/L)

The favorability of the adsorption system was assessed using the dimensionless Langmuir separation factor, R_L (Equation 15) [32]. This parameter indicates the shape of the isotherm and the nature of the sorption process. If R_L >1, the adsorption is considered unfavorable; if = 1, the isotherm is linear; if R_L = 0, the adsorption is irreversible; and if 0 < R_L < 1, the adsorption is favorable [33,34].

$$R_L = \frac{1}{1+bC_e} \quad (15)$$

where R_L is a dimensionless equilibrium parameter or separation factor, b is the constant from the Langmuir equation, and C_e the initial concentration of the selected dye-antibiotic pollutant.

2.7.2. Freundlich isotherm

The linear Freundlich isotherm was studied to model the adsorption process. The Freundlich isotherm constants, K_f and $\frac{1}{n}$, as shown in Equation 16, were determined from the plot of $\ln q_e$ against $\ln C_e$ [32,35,36].

$$\ln q_e = \frac{1}{n} \ln C_e + \log K_f \quad (16)$$

where, q_e is the amount of adsorbate absorbed at equilibrium (mg/g), K_f is the Freundlich constant (L/mg), $\frac{1}{n}$ is the Freundlich exponent (dimensionless).

2.7.3. Temkin isotherm model

The linear form of the Temkin Isotherm model is expressed in Equation 17. The plot of q_e against $\ln C_e$ was used to evaluate the constants B and A, which are the Temkin isotherm constants [37-39].

$$q_e = B \ln C_e + B \ln A \quad (17)$$

where A is the Temkin constant, B is a factor related to the heat of adsorption, and is equal to $\frac{RT}{b}$, T is the absolute temperature, and R is the universal gas constant, 8.3143 J/mol.K.

2.7.4. Dubinin-Radushkevich isotherm model

The general equation of the Dubinin-Radushkevich (D-R) isotherm model is presented in Equation 18, while the Polanyi potential (ε) is defined in Equation 19 [40]. A plot of $\ln q_e$ against ε^2 was constructed, from which the Dubinin-Radushkevich constants, β and q_{DR} were determined from the slope and intercept of the plot, respectively.

$$\ln q_e = -\beta \varepsilon^2 + \ln q_{DR} \quad (18)$$

$$\varepsilon = RT \ln \left(1 + \frac{1}{C_e}\right) \quad (19)$$

where q_e is the concentration at equilibrium, q_{DR} *and* β are Dubinin-Radushkevich constants (kJ^2/mol^2) and ε is the Polanyi potential (J/mol).

2.7.5. Jovanovich isotherm model

The linear form of the Jovanovich isotherm is expressed as Equation 20. The values of $\ln q_e$ were plotted against C_e and the constants q_{max} and K_j were evaluated from the slope and intercept, respectively [41,42].

$$\ln q_e = K_j c_e + \ln q_{max} \quad (20)$$

2.7.6. Harkin-Jura isotherm model

The Harkin-Jura model is expressed as stated in Equation 21. The Harkin-Jura constants were obtained by plotting $\frac{1}{{q_e}^2}$ against log c_e to obtain slope and intercept as - $\frac{1}{A}$ *and* $\frac{B}{A}$, respectively [40,43-46].

$$\frac{1}{{q_e}^2} = -\frac{1}{A} \log c_e + \frac{B}{A} \quad (21)$$

where B and A are Harkin-Jura constants.

3. Results and Discussion

3.1. Synthesis and Characterization of the Synthesized DRPCH

The present study reports the synthesis of a novel copolymeric hydrogel derived from DRP, a sustainable and readily available biomass material. This DRPCH demonstrated remarkable and high removal efficiency for DAM commonly found in pharmaceutical wastewater, highlighting its potential as an eco-friendly alternative to conventional treatment methods. The findings from the characterizations of DRPCH developed are presented and discussed in sections 3.1.1-3.1.4, establishing a comprehensive basis for evaluating the hydrogel's potential in environmental remediation.

3.1.1. Water absorbency capability of DRPCH

The DRPCH developed exhibited a rapid increase in water absorbency during the initial period of immersion, as shown in Figure 1. This

Copyright © 2027, ISSN: 3032-7059

was followed by a slower swelling process between 200 and 500 min, after which the hydrogel gradually approached its equilibrium swelling capacity. The rapid initial absorption may be associated with the hydrophilic functional groups present in the polymer chains, which facilitate water penetration into the hydrogel matrix. The porous structure may also provide additional pathways for water entry, while the crosslinked polymer network and its internal structural resistance regulate further diffusion and network expansion [20,23].

The maximum swelling capacities of 288% demonstrate the ability of DRPCH to absorb and retain a considerable quantity of water. This behaviour can be associated with the hydrophilic nature of the DRPCH chains and the electrostatic repulsion between ionised carboxylate groups originating from AA. These interactions promote polymer-chain expansion and facilitate the incorporation of water into the three-dimensional network. The swelling process is therefore governed by the combined effects of water diffusion, polymer-chain relaxation, osmotic pressure, and the restraining influence of the crosslinked network [47,48].

The swelling capacity of DRPCH can be further considered in relation to the findings of Zhu *et al.*, who developed a poly(acrylic acid-acrylamide/fly ash) composite hydrogel. Their material exhibited water absorption capacities of 976 g/g in distilled water and 81 g/g in 0.9% NaCl solution [20]. Although these values are considerably higher than the 288% recorded for DRPCH, the difference may be associated with variations in polymer composition, composite structure, crosslinking conditions, and experimental procedures. The comparison nevertheless demonstrates that the incorporation of different reinforcing materials and modifications to hydrogel composition can substantially influence water absorption performance.

The swelling kinetics of DRPCH also revealed that approximately 80% of its total water uptake occurred within the first two hours of immersion. The gradual reduction in the swelling rate after the initial absorption period may be attributed to the increasing resistance to further expansion as the polymer network becomes progressively hydrated. The swelling process involves the diffusion of water molecules into the hydrogel matrix, followed by polymer-chain relaxation and expansion. Equilibrium swelling is approached when the driving forces responsible for water uptake are balanced by the elastic retractive forces of the crosslinked polymer network [47,48]. The observed swelling behaviour indicates that DRPCH combines relatively rapid initial water absorption with a gradual approach to equilibrium, properties that may be beneficial in applications involving aqueous pollutant adsorption.

3.1.2. Water retention capability of DRPCH

The water retention assessment revealed that DRPCH maintained its hydrated state for approximately seven hours before significant deswelling occurred. As shown in Figure 2, its water-holding capacity gradually decreased with increasing time. This behaviour suggests that, although the hydrogel initially absorbs a considerable quantity of water, some of the absorbed water is progressively released as the polymer network undergoes deswelling. Such behaviour may be influenced by water diffusion out of the hydrogel matrix, polymer-network contraction, and changes in the interactions between water molecules and hydrophilic functional groups.

The observed retention period can be compared with findings reported for other biomass-based and chemically modified hydrogels. Hou *et al.* developed a hemicellulose-based hydrogel reinforced with chitosan and iron ions. Their hydrogel exhibited a water retention ratio of approximately 97.54% after 48 h in soil, demonstrating the effectiveness of network reinforcement and structural modification in

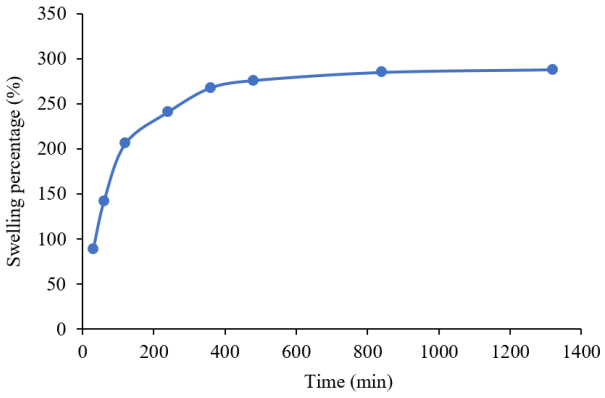


Figure 1. Water absorbency behavior of DRPCH.

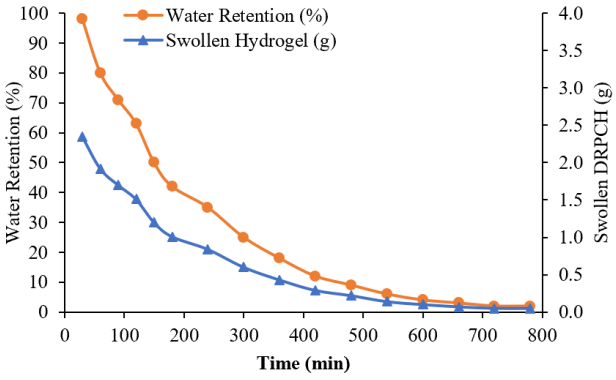


Figure 2. Water retention capacity of DRPCH.

Copyright © 2027, ISSN: 3032-7059

improving water retention [24]. Lan *et al.* also investigated the osmotic-responsive behaviour of a chitosan-catechol hydrogel in physiological saline. They reported that the hydrogel reached deswelling equilibrium after approximately 12 h, with a water retention ratio of about 25.5%. However, when tested in culture medium, the hydrogel exhibited a substantially higher equilibrium water retention ratio of approximately 69.7% [49]. These findings demonstrate that hydrogel water retention is strongly influenced by the surrounding medium and its ionic composition

Water retention measurements conducted in soil, physiological saline, culture medium, and other aqueous environments are not directly equivalent. Consequently, the differences in reported retention periods do not necessarily indicate differences in intrinsic hydrogel performance alone. The water retention behaviour of DRPCH may also be influenced by its porous structure and the stability of its crosslinked polymer network. The presence of hydrophilic functional groups promotes interactions with water molecules, while the crosslinked structure provides a framework that limits excessive network dissolution and supports the retention of absorbed water.

The gradual reduction in water-holding capacity indicates that the network cannot completely prevent water loss over prolonged periods. The ability of DRPCH to maintain hydration for several hours may be advantageous in wastewater treatment processes involving aqueous pollutant adsorption. Maintaining a hydrated polymer network may help preserve access to functional groups and adsorption sites. The practical suitability of the material will also depend on pollutant adsorption kinetics, the stability of the hydrogel during treatment, and its performance under the actual wastewater conditions [50]. The observed water retention behaviour, together with its water absorption capacity, supports further investigation of DRPCH as a potential biomass-derived adsorbent.

3.1.3. Proximate properties of raw DRP and DRPCH samples

The results of the proximate analysis of both the raw DRP and the synthesized DRPCH samples are presented in Table 1. The two samples exhibited low moisture and ash contents, moderate volatile matter, and high fixed carbon content, all of which are desirable characteristics of adsorbent for adsorption applications. The moisture content ranged from 3.55-5.90%, volatile matter ranged from 14.85-25.20%, fixed carbon ranged from 63.30-77.95%, and ash content ranged from 3.65-5.60%. The values obtained for moisture and ash content are in agreement with the recommended standards of less than 8% for adsorbent precursors, confirming that DRP-derived hydrogel meets the requirements for use as an effective adsorbent [51,52].

The low moisture content observed enhance stability and improve adsorption capacity, as excess moisture in adsorbents typically reduces efficiency by blocking adsorption sites and decreasing surface activity. Similarly, the ash content (3.65-5.60%) was below 6%, which is favorable since ash represents non-combustible mineral residues that often reduce the number of available active sites. High ash content can mask or block adsorption sites and, at the same time, reduce the percentage of fixed carbon [25,52]. The low ash levels in the present study, suggest fewer mineral impurities and a higher concentration of active carbon sites suitable for pollutant uptake. The moisture content of the DRPCH, as shown in Table 1, was lower than that of the raw pods reported by other authors [52-54].

The high fixed carbon content (63.30% and 77.95% for raw DRP and DRPCH, respectively) reflects the amount of solid carbonaceous matter available after the removal of moisture, volatiles, and ash content. High fixed carbon ensures greater stability, enhanced surface reactivity, and suitability for applications involving adsorption and pollutant capture [26]. The moderate proportion of volatile matter (14.85% and 25.20%

Table 1. Proximate analysis of the raw DRP and DRPCH samples. ND -Not Determined, MCB - Maize Cob Biochar, and DRS - Delonix regia Seed

Samples	Moisture content	Volatile matter	Fixed carbon	Ash content	References
DRP	9.90	28.00	55.80	6.12	[26]
MCB	8.93	31.00	48.50	20.50	[52]
DRP	2.73	ND	ND	ND	[53]
DRP	6.29	91.30	0.63	1.78	[54]
DRS	5.26	92.54	0.34	1.86	[54]
Raw DRP	5.90	25.20	63.30	5.60	This study
DRPCH	3.55	14.85	77.95	3.65	This study

Copyright © 2027, ISSN: 3032-7059

for DRPCH and raw DRP, respectively) further supports adsorption potential, since volatile compounds contribute to pore formation during thermal treatment, thereby improving surface area and porosity [51].

The combined features of high fixed carbon, low ash, and low moisture content therefore reinforce the suitability of the prepared DRPCH as an efficient adsorbent. These findings align with earlier reports by Dada *et al.* and Iwar *et al.*, who reported similar proximate compositions for DRP-based precursors, further validating the present results [26,53]. Adekanye *et al.* reported moisture content, volatile matter, fixed carbon, and ash content values of 8.93%, 31.00%, 48.50%, and 20.50%, respectively, for maize cob biochar [52]. These results were comparable to those obtained in the present study, except that the ash content was relatively higher than that observed in this study. The proximate analysis collectively underscores the potential of DRPCH not only for wastewater treatment but for broader adsorption-related applications, given its favorable balance of low impurities, stable carbon content, and structural suitability.

3.1.4. CHNOS elemental composition of raw DRP and DRPCH samples

The elemental composition for the raw DRP were 51.21% C, 6.90% H, 1.60% N, 0.96% S, and 39.30% O. The DRPCH sample contained 51.80% C, 6.86% H, 2.06% N, 0.67% S, and 38.59% O (Table 2). The slight increase in carbon content observed in the DRPCH, can be attributed to the incorporation of carbon-rich monomers (AA and AM) during the graft copolymerization process. This confirms successful grafting of the AA and AM onto the DRP backbone and aligns with earlier findings by Krotz and Giazzi and Yahya *et al.* [55,56]. The results obtained in this research are in agreement with those determined by Oluwasina *et al.* and Krotz and Giazzi [54,55].

The increase in carbon suggests a more carbonaceous material, which is desirable for adsorption applications, due to the potential for stronger π-π interactions with organic pollutants. The increase from 1.60 to 2.06% recorded for nitrogen content can be linked to the incorporation of acrylamide, which introduced amide groups into the DRPCH structure. The increase not only confirmed effective grafting but also introduced NH_2 functional groups, which are relevant to adsorption. These groups act as binding sites through electrostatic interactions, hydrogen bonding, or complexation with pollutants, that enhanced the adsorption efficiency of the DRPCH. Sulphur content decreased from 0.96 to 0.67%, which can be explained by the transformation of sulphur-containing compounds during synthesis.

Ammonium persulphate, used as an initiator, undergoes decomposition during the polymerization process, which facilitates grafting but does not remain in appreciable amounts in the final product. The sulphur levels obtained are consistent with the recommended values for biomass materials (0.50-0.70 wt.% or below), as reported by Yahya *et al.* [56]. The low sulphur content minimizes the potential release of sulphur oxides during the adsorption processes, thereby reducing environmental impact. Oxygen content decreased from 39.30 to 38.59%, which reflects the compositional rebalancing that occurs upon incorporation of carbon- and nitrogen-rich monomers and cross-linking agent. It further indicates structural modification of the polymer matrix.

The CHNOS elemental analysis confirms the successful chemical modification of DRP through graft copolymerization, evidenced by the enrichment of carbon and nitrogen and the controlled reduction of sulphur [57]. These changes validate the formation of DRPCH with improved surface functionality, stability, and environmental compatibility. The low sulphur and nitrogen levels in both raw DRP and DRPCH importantly suggested that only limited amounts of gaseous by-products would be released during adsorption processes, which enhances the environmental safety of the material [57]. The elemental composition collectively underscores the potential of DRPCH as a sustainable and functional adsorbent for wastewater treatment.

Table 2. CHNOS elemental analysis of the raw DRP and DRPCH samples. (NA -Not available)

S/N	Elemental	Composition % (dry weight basis)		References (1)	References (2)
		Raw DRP (%)	DRPCH (%)	Oluwasina *et al.* [54]	Krotz and Giazzi [55]
1	Carbon	51.21	51.80	45.00	61.12
2	Hydrogen	6.90	6.86	5.61	2.63
3	Nitrogen	1.60	2.06	0.13	3.49
4	Sulphur	0.96	0.67	1.69	3.93
5	Oxygen	39.30	38.59	NA	20.25
6	Sulphur / Oxygen	0.03	0.02	NA	NA

Copyright © 2027, ISSN: 3032-7059

3.2. Optimization of Dye-Antibiotics Mixture Result

The optimization of the selected DAM using the IOCEDM was effectively achieved, confirming the suitability of this statistical design for assessing component interactions while minimizing experimental runs. The optimized conditions obtained through IOCEDM led to a reliable estimation of the adsorption capacity of the synthesized DRPCH in batch experiments. The findings revealed that DRPCH maintained a high removal efficiency across the optimized DAM composition, indicating its strong surface heterogeneity and abundance of functional groups that support simultaneous adsorption of different pollutants [58]. This demonstrates that DRPCH can effectively handle multicomponent pollutant systems similar to real-life pharmaceutical wastewater conditions. The application of IOCEDM furthermore enhanced model accuracy, reduced experimental redundancy, and provided a robust statistical framework for scaling up adsorption studies [59]. The results confirm that the integration of IOCEDM not only streamlined the optimization process but also validated its potential as a multifunctional adsorbent suitable for practical wastewater treatment applications.

3.3. Batch Adsorption of DAM onto DRPCH Developed

The effects of the initial concentration and contact time on the adsorption of DAM from SPW using copolymeric hydrogel derived from *Delonix regia* pods were studied. At equilibrium, a relationship exists between the concentration of the species in solution and the concentration of the same species in the adsorbed state.

3.3.1. Effect of time on batch adsorption of DAM onto DRPCH developed

DRPCH achieved adsorption capacities of 1.9219, 1.8148, 1.9275, 1.9058, 1.9139, and 1.8828 mg/g for AMO, AMP, TETRA, TARTRA, ERY, and BRIL, respectively, at lower concentrations (20 mg/L). The corresponding maximum removal efficiencies reached were 96.09, 90.74, 96.38, 95.29, 95.70, and 94.14%, as shown in Figures 3 and 4. Adsorption capacities increased to 9.6510, 9.0963, 9.7412, 9.4773, 9.5341, and 9.2345 mg/g for the same adsorbate at higher concentrations (100 mg/L). The results clearly showed that the adsorption capacity increased with increasing initial concentration. The adsorption trends reflect the higher driving force for mass transfer at elevated solute levels, demonstrating the strong affinity and high adsorption potential of DRPCH across a wide concentration range.

The effect of time revealed that the percentage removal increased rapidly within the first 100 min, after which equilibrium was gradually approached. This trend suggests that adsorption initially occurred on the readily available active sites of DRPCH, which were quickly saturated by DAM molecules. The rate of adsorption slowed as equilibrium was attained, indicating that only a limited number of active sites remained available and that the process became diffusion controlled. The strong initial uptake highlights the effective interaction between the hydrogel's functional groups and the adsorbate molecules.

3.3.2. Effect of concentration on batch adsorption of DAM onto DRPCH

The change in adsorption capacity and percentage removal with varying initial

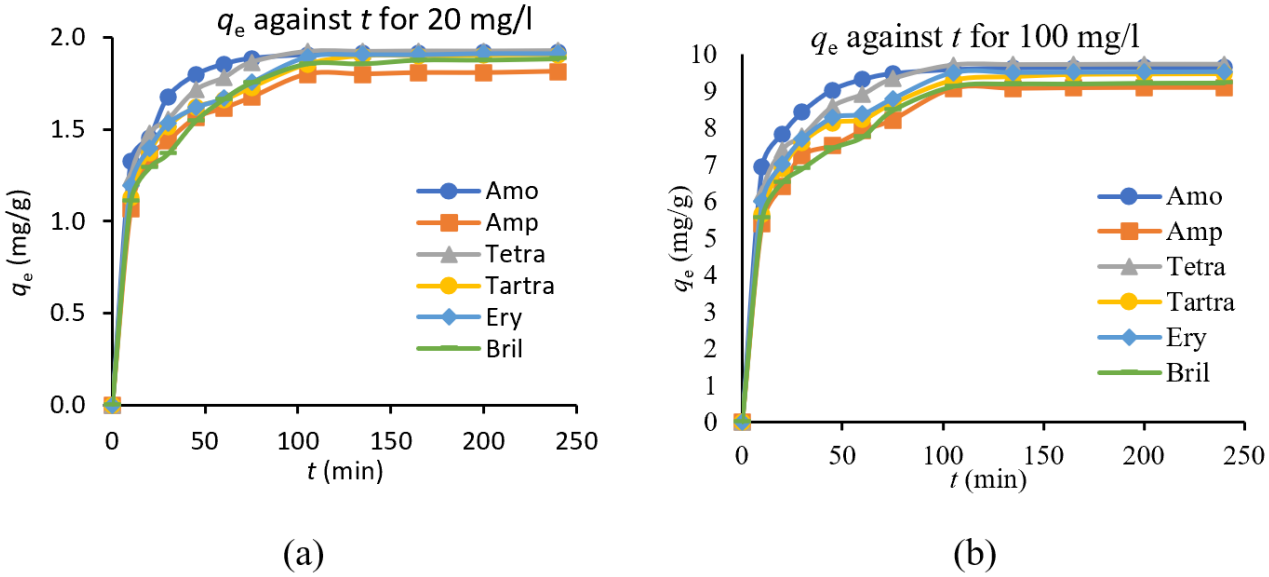


Figure 3. Adsorption capacity of DAM on DRPCH at (a) 20 mg/L and (b) 100 mg/L.

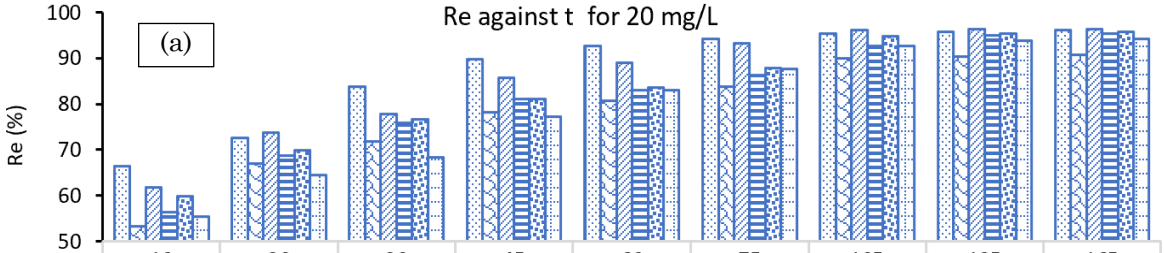
Copyright © 2027, ISSN: 3032-7059

concentrations is shown in Figure 5. The highest adsorption capacities of 9.6875, 9.2519, 9.7681, 9.4513, 9.5490, and 9.2966 mg/g were obtained for AMO, AMP, TETRA, TARTRA, ERY, and BRIL, respectively, while the corresponding highest removal efficiencies were 96.88, 92.52, 97.68, 94.51, 95.49, and 92.97%, respectively, observed at the highest concentration of 100 mg/L. The lowest values were 1.9115, 1.8370, 1.9317, 1.8669, 1.9021, and 1.8621 mg/g for AMO, AMP, TETRA, TARTRA, ERY, and BRIL, respectively, while their lowest removal efficiency of 95.57, 91.85, 96.58, 93.34, 95.10, and 93.10% recorded at 20 mg/L.

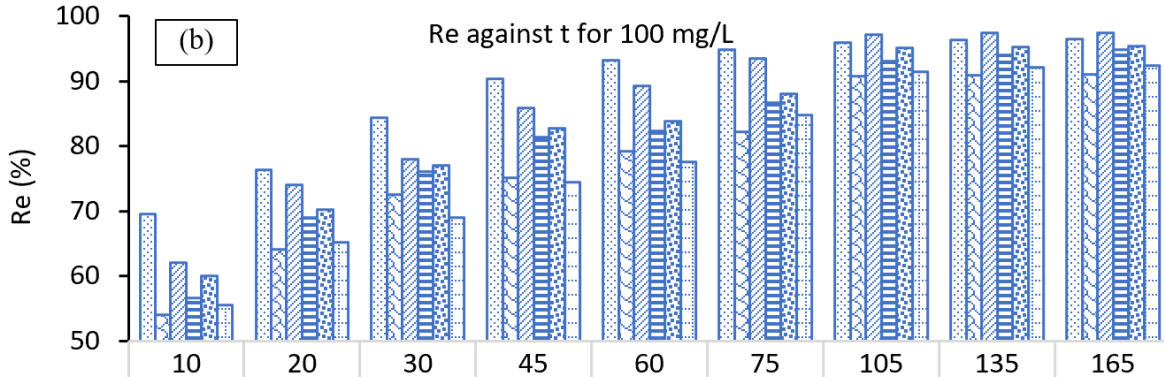
Previous research has shown that an increase in initial concentration enhances better adsorption performance. Dada *et al.* and Sazali *et al.* reported a similar trend [26,60]. The actual amount of DAM adsorbed per unit mass of adsorbent, based on the results shown in Figure 5, increased with increased concentration. The ratio of surface-active sites to the total DAM in terms of available active sites is high at low adsorbate concentration. Hence, the DAM interacts with the adsorbent to occupy the active sites on the DRPCH surface, which can be removed from the solution [26,61].

3.4. Isotherm Parameters for the Adsorption of DAM onto DRPCH

Adsorption is an equilibrium process influenced by the physicochemical properties of the adsorbent, the nature of the adsorbate, and



	10	20	30	45	60	75	105	135	165
Amo	66.41	72.66	83.85	89.84	92.71	94.27	95.31	95.83	96.09
Amp	53.33	67.04	71.85	78.15	80.74	83.70	90.00	90.37	90.74
Tetra	61.80	73.81	77.74	85.71	89.03	93.27	96.17	96.27	96.38
Tartra	56.33	68.67	75.81	81.01	82.95	86.36	92.69	94.97	95.29
Ery	59.79	69.88	76.71	81.01	83.53	87.83	94.81	95.40	95.70
Bril	55.52	64.48	68.28	77.24	83.10	87.59	92.76	93.79	94.14



	10	20	30	45	60	75	105	135	165
Amo	69.53	76.30	84.38	90.36	93.18	94.79	95.89	96.30	96.51
Amp	54.07	64.07	72.59	75.19	79.26	82.22	90.74	90.89	90.96
Tetra	62.01	74.02	77.95	85.92	89.23	93.48	97.20	97.35	97.41
Tartra	56.66	68.99	76.14	81.33	82.31	86.69	93.02	93.99	94.77
Ery	60.09	70.18	77.00	82.79	83.83	87.98	95.10	95.25	95.34
Bril	55.52	65.17	68.97	74.48	77.59	84.83	91.38	92.07	92.34

Figure 4. Re of DAM on the DRPCH at (a) 20 mg/L and (b) 100 mg/L.

Copyright © 2027, ISSN: 3032-7059

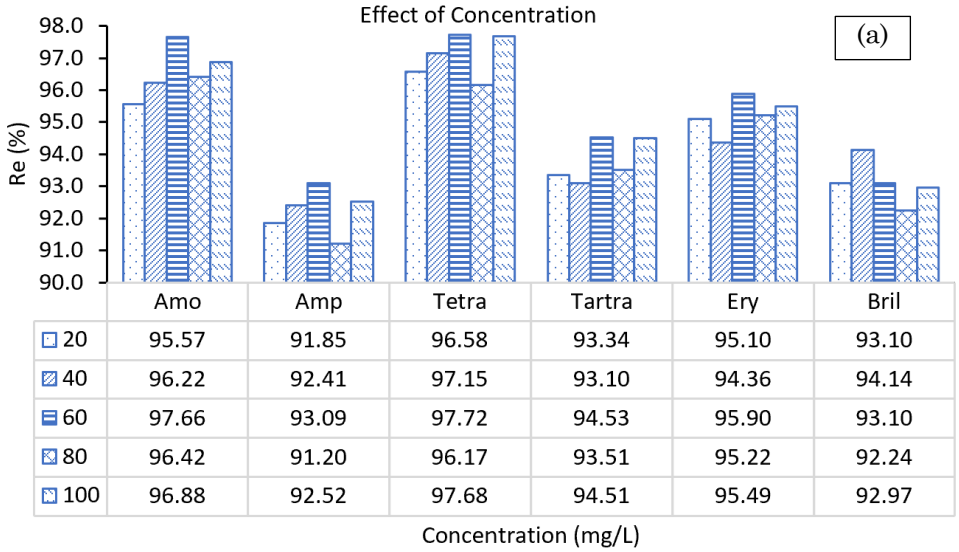
the operating conditions [62]. In this study, the adsorption equilibrium of the six selected pollutants, namely amoxicillin, ampicillin, tetracycline, tartrazine, erythrosine, and brilliant blue, onto DRPCH was investigated using six adsorption isotherm models: Langmuir, Freundlich, Temkin, Harkin–Jura, Jovanovic, and Dubinin–Radushkevich (D-R). The models were evaluated to establish their ability to describe the experimental equilibrium data and to provide insight into the possible adsorption characteristics of the DRPCH surface.

3.4.1. Langmuir isotherm model

The six linearized forms of the Langmuir isotherm were evaluated to determine their suitability for describing the adsorption of DAM onto DRPCH (Figure 6). The estimated maximum adsorption capacities (q_{max}) from the six Langmuir forms exhibited considerable variations, with both positive and negative values obtained for the different pollutants. The negative values obtained from some of the linearized forms indicate that these equations produced physically unrealistic adsorption parameters [45,62]. Such results suggest that the assumptions of the Langmuir model, particularly the representation of adsorption through equivalent and energetically uniform sites, may not adequately describe the adsorption behaviour of all the investigated pollutants on DRPCH.

The coefficients of determination obtained from Langmuir forms 1 and 2 were identical for each pollutant, with values of 0.9144, 0.9898, 0.9567, 0.9879, 0.9776, and 0.9806 for AMO, AMP, TETRA, TARTRA, ERY, and BRIL, respectively (Table 3). Among the six pollutants, AMP exhibited the highest (R^2) value (0.9898), followed by TARTRA (0.9879), BRIL (0.9806), ERY (0.9776), TETRA (0.9567), and AMO (0.9144). Although these values indicate reasonable linear correlations for Langmuir forms 1 and 2, the physically unrealistic parameters obtained from some of the other linearized forms limit the overall applicability of the Langmuir model.

The favourability of adsorption under the Langmuir assumption is commonly assessed using the dimensionless separation factor (R_L).



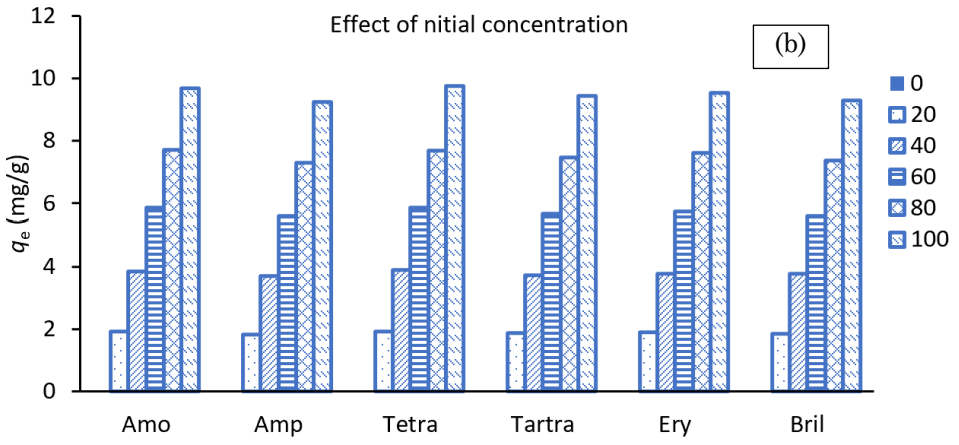


Figure 5. The plot of (a) Re and (b) q_e against the initial concentration.

Copyright © 2027, ISSN: 3032-7059

Values between 0 and 1 indicate favourable adsorption, a value of 1 indicates linear adsorption, a value greater than 1 indicates unfavourable adsorption, while a value approaching zero represents increasingly irreversible adsorption [22,63-66]. In this study, the calculated (R_L) values ranged from -14.3451 to 3.9646 (Table 4). The occurrence of negative R_L values are physically inconsistent with the conventional interpretation of the Langmuir separation factor and indicates that the corresponding Langmuir constants require further examination. Therefore, these negative values should not be interpreted directly as evidence of unfavourable adsorption. Rather, they suggest that the Langmuir model did not provide physically meaningful parameter estimates for some of the DAM-DRPCH systems.

The differences observed between the Langmuir and other isotherm models are consistent with the limitations of applying a homogeneous monolayer adsorption model to

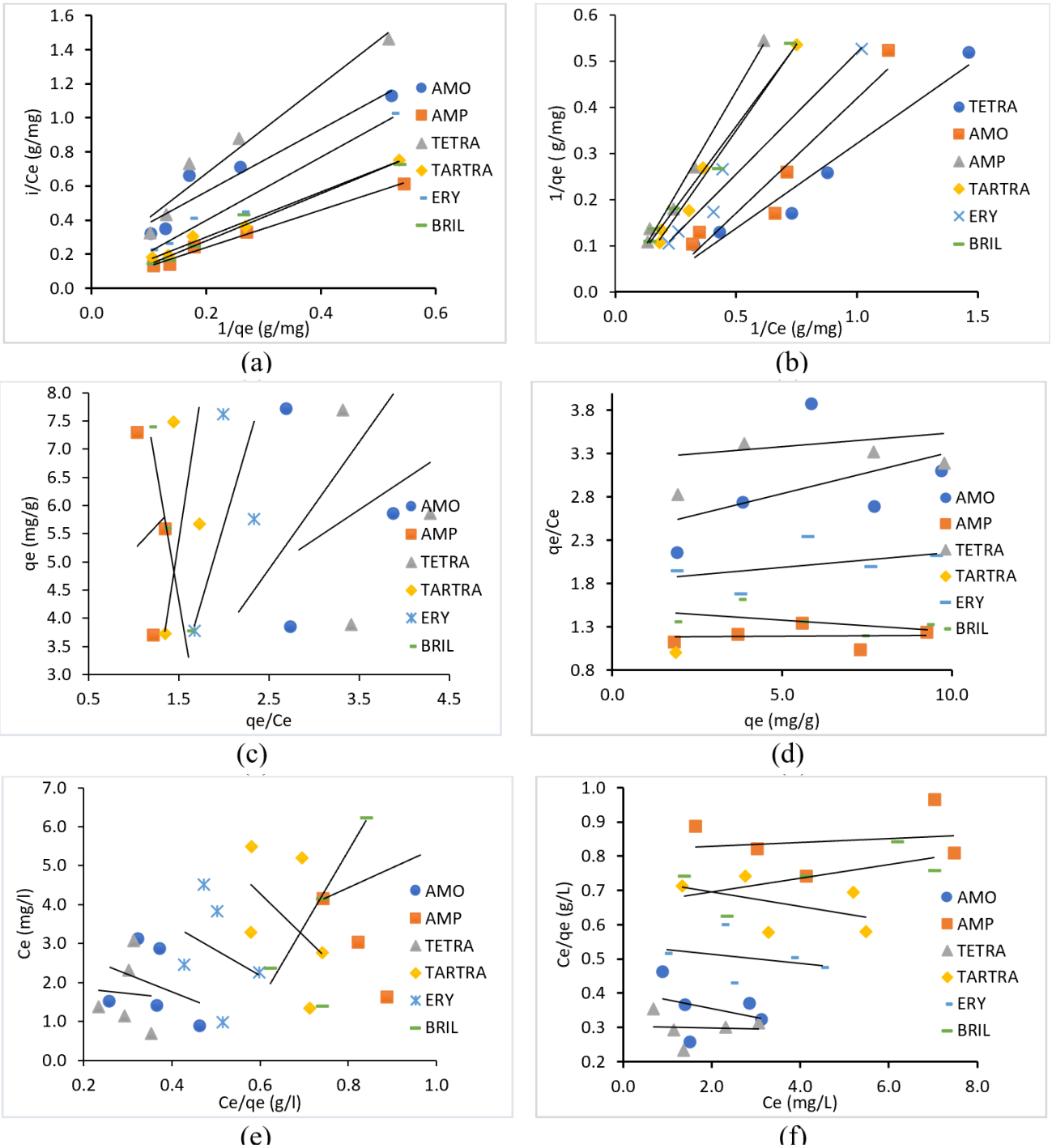


Figure 6. Adsorption isotherms plot of (a) Langmuir-1; (b) Langmuir-2; (c) Langmuir-3; (d) Langmuir-4; (e) Langmuir-5 and (f) Langmuir-6.

Copyright © 2027, ISSN: 3032-7059

structurally complex adsorbents. Adsorbents derived from biomass and modified polymeric materials may contain different functional groups and adsorption environments, which can produce non-uniform adsorption behaviour [41,63,67]. The Langmuir model may provide a reasonable statistical fit for some pollutants without necessarily representing the overall adsorption characteristics of DRPCH.

Similar trends for R_L were reported by Pandimadevi *et al.*, Wahab *et al.*, and Hani *et al.* [41,63,67]. Yaoning *et al.* and Chen *et al.* obtained 145.3 and 943.40 mg/g, and 0.9949 and 0.9900% for the values of maximum adsorption capacity and removal efficiency, respectively, in the adsorption of methylene blue [22,66]. Mansoori *et al.* obtained 370.37 mg/g and 0.8600% as the values of maximum adsorption capacity and the removal efficiency, respectively, in the adsorption of bisphenol [64]. Acharya *et al.* got 2.24-3.55 mg/g and 0.9800% for arsenic and fluoride adsorption as the values of maximum adsorption capacity and removal efficiency, respectively [65].

3.4.2. Freundlich isotherm model

The Freundlich isotherm was applied to examine the adsorption behaviour of DAM on the potentially heterogeneous surface of DRPCH (Figure 7). The Freundlich adsorption capacity constants (K_f) obtained for AMO, AMP, TETRA, TARTRA, ERY, and BRIL were 2.6188, 1.1954, 3.3121, 1.3515, 1.9063, and 1.5108 mg/g, respectively. The corresponding adsorption intensity parameters (n) were 0.8652, 1.0042, 0.9553, 0.9085, 0.9499, and 1.0922, respectively. The coefficients of determination were 0.9044, 0.9759, 0.9449, 0.9740, 0.9656, and 0.9792 for AMO, AMP, TETRA, TARTRA, ERY, and BRIL, respectively (Table 5). These values indicate that the Freundlich model provided a relatively good representation of the equilibrium adsorption data, particularly for AMP, TARTRA, ERY, and BRIL.

The Freundlich exponent ($\frac{1}{n}$) is commonly used to evaluate adsorption intensity and surface heterogeneity. Values between 0 and 1 are conventionally associated with favourable

Table 3. Parameter estimates for the Langmuir isotherm.

Linear model / Adsorbent	q_{max} (mg/g)						R^2					
	AMO	AMP	TETRA	TARTRA	ERY	BRIL	AMO	AMP	TETRA	TARTRA	ERY	BRIL
Langmuir 1	5.0787	57.4713	6.6050	28.1690	42.0168	0.0005	0.9144	0.9898	0.9567	0.9879	0.9776	0.9806
Langmuir 2	6.4083	68.7231	8.0927	31.7447	73.9718	-150.66	0.9144	0.9898	0.9567	0.9879	0.9776	0.9806
Langmuir 3	-0.7524	3.4926	2.2014	-10.3640	-5.3276	18.4060	0.2172	0.0047	0.0350	0.4096	0.1942	0.2368
Langmuir 4	24.3876	420.57	97.7356	-33.4578	51.1186	-59.667	0.2172	0.0047	0.0350	0.4096	0.1942	0.2368
Langmuir 5	-4.4840	5.0786	-1.1493	-10.9130	-6.4423	19.1930	0.1183	0.0285	0.0027	0.2328	0.0841	0.3809
Langmuir 6	-37.878	178.571	-416.67	-46.9484	-76.336	50.5051	0.1183	0.0285	0.0027	0.2328	0.0841	0.3809

Adsorbate	q_{max} (mg/g)	R^2	Reference
Methylene Blue	145.3	0.9949	[22]
Bisphenol A	370.37	0.8600	[64]
Arsenic	3.55	0.9800	[65]
Fluoride	2.24	0.9800	[65]
Methylene Blue	943.40	0.9900	[66]

Table 4. Langmuir isotherm separation factor (R_L) of DAM onto DRPCH at different concentrations.

Adsorbate	C_o (mg/L)	C_e (mg/L)	Lang 1	Lang 2	Lang 3	Lang 4	Lang 5	Lang 6
AMO	20.00	0.8854	0.9136	0.9359	1.6487	0.9213	0.8006	1.0609
	40.00	1.4063	0.9294	0.9018	2.6662	0.8805	0.7165	1.1003
	60.00	1.5104	0.9340	0.8953	3.0416	0.8728	0.7018	1.1085
	80.00	2.8646	0.9641	0.8185	-3.6627	0.7834	0.5538	1.2279
	100.00	3.1250	0.9670	0.8052	-2.5723	0.7683	0.5322	1.2539
AMP	20.00	1.6296	0.9751	0.9793	21.060	0.9955	0.1874	0.9890
	40.00	3.0370	0.9545	0.9620	-1.2901	0.9916	0.1101	0.9798
	60.00	4.1481	0.9389	0.9488	-0.7020	0.9885	0.0830	0.9726
	80.00	7.0370	0.9005	0.9162	-0.3212	0.9807	0.0507	0.9543
	100.00	7.4815	0.8949	0.9114	-0.2965	0.9795	0.0478	0.9516
TETRA	20.00	0.6832	0.9619	0.9700	2.7919	0.9780	0.7508	1.0054
	40.00	1.1387	0.9380	0.9509	-14.345	0.9639	0.6438	1.0091
	60.00	1.3665	0.9266	0.9417	-3.5254	0.9570	0.6010	1.0109
	80.00	2.3188	0.8815	0.9049	-0.8487	0.9291	0.4702	1.0187
	100.00	3.0642	0.8491	0.8781	-0.5323	0.9084	0.4018	1.0248

Copyright © 2027, ISSN: 3032-7059

adsorption, whereas values greater than 1 indicate less favourable adsorption behaviour. Based on the reported (n) values, the corresponding $\frac{1}{n}$ values range from approximately 0.9156 to 1.1558. Specifically, the values are 1.1558, 0.9958, 1.0468, 1.1007, 1.0527, and 0.9156 for AMO, AMP, TETRA, TARTRA, ERY, and BRIL, respectively. These results indicate differences in adsorption intensity among the pollutants, with BRIL showing a favourable Freundlich exponent, while the values for most of the other pollutants are close to or slightly above unity.

The Freundlich model assumes a heterogeneous adsorption surface with a non-uniform distribution of adsorption energies. Its relatively good performance in the present study suggests that the DRPCH surface may provide different adsorption environments for the investigated pollutants. This behaviour is plausible for a biomass-derived copolymeric hydrogel containing different functional groups and structural regions. Similar applications of the Freundlich model have been reported in adsorption studies involving heterogeneous adsorbent surfaces [9,22,66].

The Freundlich adsorption capacities obtained in this study can also be considered alongside the maximum adsorption capacities reported for other adsorbent systems. Yaoning *et al.* and Chen *et al.* reported maximum adsorption capacities of 145.3 and 943.40 mg/g, respectively, for methylene blue adsorption [22,66]. Mansoori *et al.* reported a maximum adsorption capacity of 370.37 mg/g for bisphenol adsorption [64], while Acharya *et al.* reported values between 2.24 and 3.55 mg/g for arsenic and fluoride adsorption [65]. These differences illustrate the influence of adsorbent composition, surface chemistry, pore structure, and adsorbate properties on adsorption capacity.

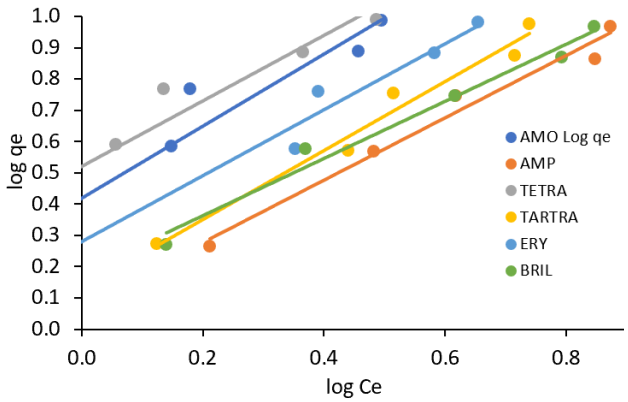


Figure 7. Freundlich isotherm plot of the adsorption of DAM onto DRPCH.

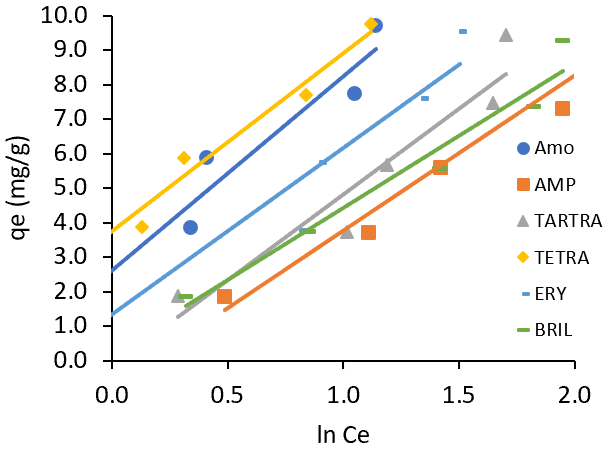


Figure 8. Temkin isotherm graph for the adsorption of DAM onto DRPCH.

3.4.3. Temkin isotherm model

The Temkin isotherm was employed to investigate the relationship between adsorbate concentration and adsorption energy during the adsorption process (Figure 8). The equilibrium binding constants (A) obtained for AMO, AMP, TETRA, TARTRA, ERY, and BRIL were 1.5939, 1.1779, 2.0705, 0.9683, 1.3189, and 1.0615 L/mg, respectively. The corresponding Temkin constants (B) were 5.6302, 4.4861, 5.1481, 4.9656, 4.8255, and 4.1820 J/mol, respectively (Table 6). The R^2 were 0.9354, 0.9442, 0.9796, 0.9067, 0.9021, and 0.9566 for AMO, AMP, TETRA, TARTRA, ERY,

Table 5. Freundlich isotherm estimated parameters.

Adsorbate	n	K_f (mg/g)	R^2	References
Tetracycline	4.1389	81.9960	0.9636	[68]
Methylene blue	0.7689	1.4570	0.9102	[53]
Nickel	0.34000	0.6600	0.9497	[9]
Tetracycline	2.7027	44.400	0.9140	[36]
Methylene blue	21.1600	108.100	0.5761	[22]
Fluoroquinolones	1.3220	3.7780	0.9517	[69]
Methylene blue	2.5660	141.95	0.8508	[66]
Moxifloxacin	1.1547	7.8890	0.9980	[71]
Amoxicillin	1.9240	3.5770	0.9849	[74]
Doripenem	2.3400	7.8460	0.9849	[74]
Ampicillin	2.6316	10.4000	0.9240	[70]
Amoxicillin	0.6150	33.7320	0.9928	[75]
Amoxicillin	0.8652	2.6188	0.9044	This study
Ampicillin	1.0042	1.1954	0.9759	This study
Tetracycline	0.9553	3.3121	0.9449	This study
Tartrazine	0.9085	1.3515	0.9740	This study
Erythrosine	0.9499	1.9063	0.9656	This study
Brilliant Blue	1.0922	1.5108	0.9792	This study

K_f and n are the Freundlich isotherm constants, R^2 is the coefficient of determination.

Copyright © 2027, ISSN: 3032-7059

and BRIL, respectively. These results indicate that the Temkin model provided a relatively good description of the adsorption equilibrium data, particularly for TETRA, which recorded the highest R^2 value of 0.9796.

The Temkin model considers the influence of adsorbate-adsorbent interactions and assumes that the heat of adsorption decreases approximately linearly with increasing surface coverage. The relatively low values of the Temkin constant obtained in this study suggest a limited variation in the adsorption energy over the investigated concentration range. The model's performance also indicates that the adsorption behaviour cannot be adequately represented by a simple description of uniform adsorption sites alone. The findings are comparable with previous adsorption studies in which the Temkin model provided a reasonable representation of adsorption equilibrium data and was used to assess the interaction between adsorbate molecules and adsorbent surfaces [68-70]. The positive A values indicate favorable binding of the adsorbate onto the adsorbent, while low B values (< 20 J/mol) signify that the adsorption is predominantly physical, involving weak electrostatic or van der Waals interactions rather than chemical bonding [76-78].

3.4.4. Dubinin-Radushkevich isotherm model

The Dubinin-Radushkevich (D-R) isotherm was applied to investigate the adsorption capacity and characteristic adsorption energy of the DRPCH system (Figure 9). The calculated D-R adsorption capacities (q_{DR}) were 11.2526, 8.2441, 10.6313, 8.4545, 8.4537, and 8.2788 mg/g for AMO, AMP, TETRA, TARTRA, ERY, and BRIL, respectively. The corresponding D-R constants (β) were 0.0337, 0.0101, 0.0202, 0.0539, 0.0337, and 0.0539, respectively. The mean adsorption energy (E) values were 3.8519, 7.0360, 4.9752, 3.0457, 3.8519, and 3.0457 kJ/mol, respectively (Table 7).

The calculated mean adsorption energies were relatively low, ranging from 3.0457 to 7.0360 kJ/mol. These values have traditionally been interpreted as being consistent with physical adsorption involving relatively weak interactions. The adsorption of DAM onto DRPCH is predominantly governed by physisorption, since all the values of E were below 8 kJ/mol, which involves weak van der Waals and electrostatic interactions [70,73].

The coefficients of determination for the D-R model were 0.9568, 0.9259, 0.9770, 0.8665, 0.8669, and 0.9464 for AMO, AMP, TETRA, TARTRA, ERY, and BRIL, respectively. These results indicate that the D-R model provided a

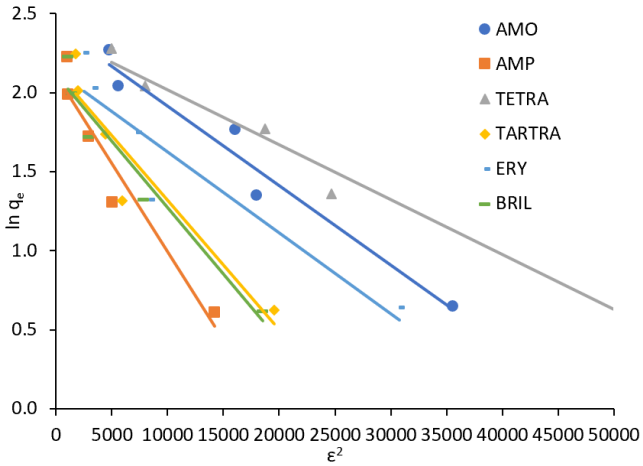


Figure 9. Dubinin-Radushkevich isotherm plot of DAM onto DRPCH.

Table 6. Temkin isotherm estimated parameters. (A and B are the Temkin isotherm constants, R² is the coefficient of determination)

Adsorbate	A (L/mg)	B (J/mol)	R^2	References
Methylene blue	0.3628	2.735	0.9919	[67]
Ofloxacin	3.280	15.27	0.9770	[41]
Azithromycin	12.25	15.68	0.7968	[72]
Phosphate	1.1900	1.8900	0.9897	[73]
Tetracycline	0.5230	38.90	0.9914	[68]
Moxifloxacin	0.6450	31.67	0.9620	[71]
Fluoroquinolones	0.9226	95.06	0.9226	[69]
Mercury	0.0020	1.2290	0.9890	[45]
Ampicillin	0.4550	14.94	0.9980	[70]
Amoxicillin	1.5939	5.6302	0.9354	This study
Ampicillin	1.1779	4.4861	0.9442	This study
Tetracycline	2.0705	5.1481	0.9796	This study
Tartrazine	0.9683	4.9656	0.9067	This study
Erythrosine	1.3189	4.8255	0.9021	This study
Brilliant Blue	1.0615	4.1820	0.9566	This study

Table 7. Dubinin-Radushkevich isotherm estimated parameters. (β and q_{DR} are the Dubinin-Radushkevich constants and R^2 is the coefficient of determination).

Adsorbent / Adsorbate	q_{DR} (mg/g)	β kJ/mol^2	E (kJ/mol)	R^2	References
Azithromycin	76.1000	2.0×10^{-7}	1.5810	0.8023	[72]
Tetracycline	39.5000	7.29×10^{-4}	26.200	0.7500	[36]
Phosphate		2.84×10^{-7}	1.3500	0.9351	[73]
Amoxicillin	38.793	0.084	32.110	0.9849	[74]
Doripenem	55.256	0.093	87.228	0.9849	[74]
Moxifloxacin	29.9800	1.98×10^{-9}	15.140	0.9340	[71]
Mercury	14.5640	0.2760	1.3450	0.8920	[45]
Amoxicillin	11.2526	0.0337	3.8519	0.9568	This study
Ampicillin	8.2441	0.0101	7.0360	0.9259	This study
Tetracycline	10.6313	0.0202	4.9752	0.9770	This study
Tartrazine	8.4545	0.0539	3.0457	0.8665	This study
Erythrosine	8.4537	0.0337	3.8519	0.8669	This study
Brilliant	8.2788	0.0539	3.0457	0.9464	This study

Copyright © 2027, ISSN: 3032-7059

good description of the adsorption equilibrium data for some of the pollutants, particularly AMO and TETRA. The relatively high R^2 values suggest that the model can provide useful information about the adsorption behaviour of these systems, although its predictive performance varies among the pollutants.

The D-R results are consistent with the general observation that adsorption behaviour may involve different interaction energies depending on the chemical characteristics of the adsorbate and the adsorption environment. The D-R results in comparison with the Temkin isotherm model, which indicated a low heat of adsorption (B = 4-65 J/mol) and suggested a physical adsorption process, further confirming the dominance of physisorption as the controlling adsorption mechanism [70,73]. Both models support that the adsorption of the DAM occurs mainly through weak physical interactions rather than strong chemical bonding, consistent with the earlier interpretation of a surface process involving electrostatic attraction and van der Waals forces.

3.4.5. Jovanovich isotherm model

The Jovanovic isotherm was employed to further examine the adsorption equilibrium characteristics of DAM onto DRPCH (Figure 10). The calculated Jovanovic equilibrium constants (K_j) were 0.5912, 0.2376, 0.6035, 0.3555, 0.4418, and 0.2492 L/mg for AMO, AMP, TETRA, TARTRA, ERY, and BRIL, respectively. The corresponding maximum adsorption capacities (q_{max}) were 1.5604, 1.5853, 1.7971, 1.3541, 1.4353, and 1.6944 mg/g, respectively (Table 8). The corresponding R^2 were 0.8165, 0.8954, 0.8290, 0.9303, 0.9239, and 0.9109 for AMO, AMP, TETRA, TARTRA, ERY, and BRIL, respectively, indicating the formation of a stable adsorbate layer on the DRPCH surface. These results indicate moderate agreement between the experimental data and the Jovanovic model, with relatively better fits for TARTRA, ERY, and BRIL.

The calculated maximum adsorption capacities were comparable to some values reported for other biomass-derived adsorbents. Amole *et al.* reported a maximum adsorption capacity of 1.0783 mg/g for nitrophenol adsorption using groundnut-shell-based adsorbents, whereas Nandiyanto *et al.* reported a higher value of 10.7299 mg/g for mercury adsorption using rice-husk-derived materials [42,45]. The differences in adsorption capacities may be associated with variations in adsorbent surface chemistry, structural properties, and the physicochemical characteristics of the adsorbates.

The Jovanovic model incorporates the possibility of mechanical interactions between the adsorbate and adsorbent [42]. Its performance in this study suggests that it can provide an additional description of the adsorption equilibrium behaviour. The moderately high R^2 values indicate that adsorption proceeds through monolayer coverage with minimal chemisorptive involvement, consistent with the low adsorption energy (E < 8 kJ/mol) derived from the D-R model and the low Temkin B values, which reflect weak adsorbate-adsorbent interactions. Therefore, the Jovanovich model reinforces the conclusion that the adsorption of DAM onto DRPCH is primarily governed by physical adsorption dominated by van der Waals and electrostatic forces.

3.4.6. Harkin-Jura isotherm

The Harkin-Jura isotherm was used to examine the possibility of multilayer adsorption on a heterogeneous adsorbent surface (Figure 11).

Table 8. Jovanovich isotherm estimated parameters. (K_j is the Jovanovich equilibrium constant, q_{max} is the Maximum adsorption capacity)

Adsorbate	K_j (L/mg)	q_{max} (mg/g)	R^2	References
Ofloxacin	-0.0090	24.0420	0.7750	[41]
Nitrophenol	0.0914	1.0783	0.8980	[42]
Mercury	-0.0060	10.7299	0.9990	[45]
Maize Cob	0.0348	13.1615	0.9082	[79]
Amoxicillin	0.5912	1.5804	0.8165	This study
Ampicillin	0.2376	1.5853	0.8954	This study
Tetracycline	0.6035	1.7971	0.8290	This study
Tartrazine	0.3555	1.3541	0.9303	This study
Erythrosine	0.4418	1.4353	0.9239	This study
Brilliant Blue	0.2492	1.6944	0.9109	This study

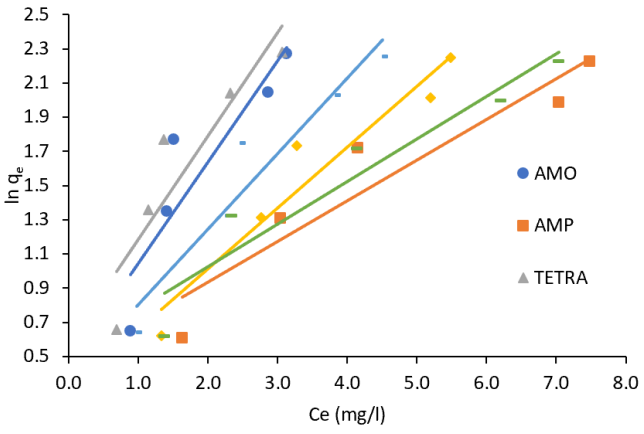


Figure 10. Jovanovich isotherm plot for the adsorption of DAM onto DRPCH.

Copyright © 2027, ISSN: 3032-7059

The calculated model parameters were 2.5025, 0.4444, and 0.6829 for AMO; 2.5471, 0.8268, and 0.8082 for AMP; 2.8385, 0.3974, and 0.6999 for TETRA; 2.2994, 0.6999, and 0.8737 for TARTRA; 2.4667, 0.5942, and 0.8821 for ERY; and 2.8802, 0.7958, and 0.7839 for BRIL, respectively. The corresponding coefficients of determination ranged from 0.6829 to 0.8821 (Table 9). Compared with the other isotherm models, the Harkin-Jura model generally exhibited lower R^2 values, indicating a relatively weaker representation of the experimental equilibrium data.

The model is commonly associated with multilayer adsorption on heterogeneous surfaces with non-uniform pore distributions. Similar trends were observed and reported by Abiodun *et al.*, Nandiyanto *et al.*, and Karim *et al.*, who noted that the Harkin-Jura model generally supports the occurrence of multilayer adsorption but rarely offers the best statistical fit compared to the Freundlich or Temkin models [44-46]. The present results therefore suggest that, although surface heterogeneity and possible multilayer interactions may contribute to the adsorption process, the Harkin-Jura model is not the most appropriate mathematical representation of the equilibrium data obtained for DRPCH.

3.4.7. Selection of a suitable isotherm model

The suitability of the investigated adsorption isotherm models was evaluated primarily using their coefficients of determination. The average R^2 values obtained were 0.9573 for the Freundlich model, 0.9374 for the Temkin model, 0.9233 for the Dubinin-Radushkevich model, 0.8843 for the Jovanovic model, and 0.7885 for the Harkin-Jura model (Table 10). Based on these average values, the overall order of model performance was in the order of Freundlich (0.9573) >Temkin (0.9374) >Dubinin-Radushkevich (0.9233) >Jovanovich (0.8843) >Harkin-Jura (0.7885). The Freundlich model therefore provided the best overall representation of the experimental adsorption equilibrium data. Its superior average R^2 value suggests that adsorption of the investigated pollutants onto DRPCH is better described by a heterogeneous adsorption model than by a uniform monolayer adsorption model. This interpretation is consistent with the expected structural and chemical complexity of a biomass-derived copolymeric hydrogel, which may contain adsorption sites with different chemical environments and interaction energies.

Generally, high R^2 values close to unity across most of the models imply that the

Table 9. Harkin-Jura isotherm estimated parameters. (A and B are the Harkin-Jura constants)

Adsorbates	A (mg²/g²)	B (mg²/g²)	R^2
Amoxicillin	2.5025	0.4444	0.6829
Ampicillin	2.5471	0.8268	0.8082
Tetracycline	2.8385	0.3974	0.6999
Tartrazine	2.2994	0.6999	0.8737
Erythrosine	2.4667	0.5942	0.8821
Brilliant Blue	2.8802	0.7958	0.7839

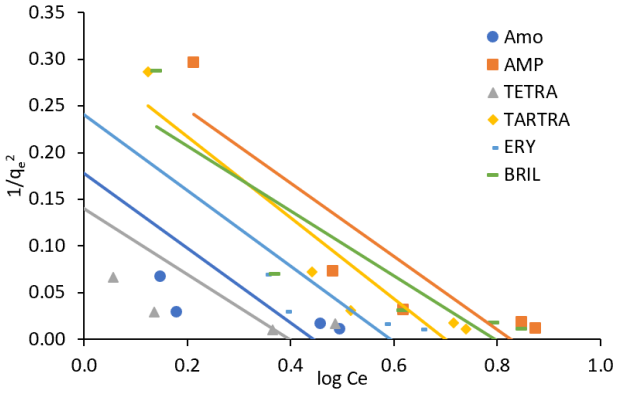


Figure 11. Harkin-Jura isotherm plot of selected DAM onto DRPCH.

Table 10. Suitable isotherm models and their parameters. (D-R- Dubinin-Radushkevich, H-J- Harkin-Jura, Ave R^2- Average R^2)

Model	Freundlich	Temkin	D-R	Jovanovich	H-J	Ave R^2
AMO	0.9044	0.9354	0.9568	0.8165	0.6829	0.8592
AMP	0.9759	0.9442	0.9259	0.8954	0.8082	0.9099
TETRA	0.9449	0.9796	0.9770	0.8290	0.6999	0.8861
TARTRA	0.9740	0.9067	0.8665	0.9303	0.8737	0.9102
ERY	0.9656	0.9021	0.8669	0.9239	0.8821	0.9081
BRIL	0.9792	0.9566	0.9464	0.9109	0.7839	0.9154
Ave R^2	0.9573	0.9374	0.9233	0.8843	0.7885	

Copyright © 2027, ISSN: 3032-7059

adsorption process was favourable and that the equilibrium data were well represented by the applied isotherm equations. The Langmuir models were excluded from this comparison because some of their isotherm constants were extremely small and could not adequately describe the adsorption process. The most suitable model varied among the individual pollutants. For AMO, the D-R model provided the best fit, followed by Temkin, Freundlich, Jovanovic, and Harkin-Jura. For AMP and BRIL, the Freundlich model exhibited the best fit, followed by Temkin, D-R, Jovanovic, and Harkin-Jura. The adsorption of TETRA was best represented by the Temkin model, followed by D-R, Freundlich, Jovanovic, and Harkin-Jura. For TARTRA and ERY, the Freundlich model provided the best fit, followed by Jovanovic, Temkin, Harkin-Jura, and D-R. These differences indicate that the adsorption equilibrium behaviour of DRPCH is influenced by the physicochemical characteristics of the individual pollutants. Although the Freundlich model provides the best overall statistical representation, the performance of the other models for particular pollutants suggests that different adsorption interactions may contribute to the observed equilibrium behaviour.

The Freundlich model is considered the most appropriate among the investigated models for describing the combined adsorption behaviour of DAM onto DRPCH. The use of multiple isotherm models is particularly important because no single model universally describes all adsorption systems. These results are consistent with previous reports by Abiodun *et al.*, Nandiyanto *et al.*, and Karim *et al.* who observed that the Freundlich and Temkin models effectively describe adsorption processes involving complex pollutant mixtures on heterogeneous bio-based adsorbents [44-46].

4. Conclusions

This study investigated the adsorption equilibrium behaviour of DRPCH for the removal of selected dyes and antibiotics from synthetic pharmaceutical wastewater under batch conditions. The adsorption experiments demonstrated that DRPCH effectively removed the six selected pollutants, with maximum adsorption capacities ranging from 9.10 to 9.74 mg/g and removal efficiencies of 90.96-97.41%. The experimental equilibrium data were evaluated using six adsorption isotherm models. Among these models, the Freundlich isotherm provided the best overall fit, with an average R^2 of 0.9573, indicating that it was the most appropriate model for describing the overall adsorption equilibrium behaviour of the investigated pollutants onto DRPCH. However, the suitability of individual models varied with the pollutant, with the D-R model providing the best fit for amoxicillin and the Temkin model for tetracycline. The adsorption parameters further suggested variations in adsorption behaviour depending on the physicochemical characteristics of the individual pollutants. The findings establish DRPCH as a promising copolymeric hydrogel for the adsorption-based removal of selected pharmaceutical and dye pollutants from aqueous solutions under batch conditions. Its high adsorption capacity and favourable isotherm performance collectively highlight its potential as a practical and sustainable material for real-world wastewater treatment applications.

Acknowledgement

The authors gratefully acknowledge the Tertiary Education Trust Fund (TETFund), Ladoke Akintola University of Technology (LAUTECH), Ogbomoso Branch, for providing the financial support that made this research possible. The authors also appreciate the Bioenvironmental, Water and Engineering Research Group (BWERG), LAUTECH, Ogbomoso, for its support and valuable contributions throughout the research. Special thanks are extended to the laboratory personnel of Al-Hikmah University, Ilorin, for their technical assistance and support during the experimental work.

CRedit Authors Statement

Author Contributions: Ilesanmi A. Ojo initiated the study, developed the research methodology, conducted the investigation, carried out the data analysis, and prepared the initial manuscript. Ayobami O. Ajani contributed to the experimental investigation, and manuscript review. Ibrahim O. Tijani participated in the development of the methodology, and experimental work. Akeem O. Olayiwola contributed to the provision of research resources, validation of results, and manuscript revision. Aminat A. Adetayo-Balogun assisted with the validation, and review of the manuscript. Abass O. Alade provided research supervision, critically evaluated the manuscript, made substantial corrections, and contributed to its revision and final refinement. All authors have read and agreed to the published version of the manuscript.

Declaration of Generative AI Use

The authors confirm that no AI-assisted technologies were used in the preparation, writing and editing of this manuscript.

Copyright © 2027, ISSN: 3032-7059

Conflict of Interest Statements

The authors declare that there is no conflict of interest regarding the publication of this work.

References

[1] Fomnya, H.J., Ngulde, S.I., Amshi, K.A., Bilbonga, G. (2021). Antibiotics: Classifications and mechanisms of resistance. *International Journal of Applied Microbiology and Biotechnology Research, 9*(15), 38-50. DOI: 10.33500/ijambr.2021.09.004

[2] Askalany, A., Ali, E.S., Mohammed, R.H. (2020). A novel cycle for adsorption desalination system with two stages, an ejector for higher water production and efficiency. *Desalination*, *496*, 47-53. DOI: 10.1016/j.desal.2020.114753

[3] Wang, X., Gao, Y., Jiang, X., Zhang, Q., Liu, W. (2021). Analysis on the Characteristics of Water Pollution Caused by Underground Mining and Research Progress of Treatment Technology. *Advances in Civil Engineering, 10(11)*, 1-14. DOI: 10.1155/2021/9984147

[4] Carrascal-Hernández, D., Orozco-Beltrán, E., Insuasty, D., Márquez, E., Grande-Tovar, C. (2025). Systematic evaluation of biodegradation of azo dyes by microorganisms: efficient species, physicochemical factors, and enzymatic systems. *International Journal of Molecular Sciences, 26* (16), DOI: 10.3390/ijms26167973.

[5] Bassem, S.M. (2020). Water pollution and aquatic biodiversity. *Biodiversity International Journal,* 4(1), 10-16. DOI: 10.15406/bij.2020.04.00159

[6] Al-Harby, N.F., Albahly, E.F., Mohamed, N.A. (2021). Kinetic, isotherm and thermodynamic studies for efficient adsorption of Congo Red dye from aqueous solution onto novel cyanoguanidine modified chitosan adsorbent. *Polymers*, *13*(24), 44-56. DOI: 10.3390/polym13244446

[7] Ajala, A., Akinnawo, O., Bamisaye, A., Adedipe, T., Adesina, O., Okon-Akan, A., Bello, S. (2023). Adsorptive removal of antibiotic pollutants from wastewater using biomass/biochar-based adsorbents. *Royal Society of Chemistry Advances,* 13(7), 4678-4712. DOI: 10.1039/D2RA06436G

[8] Peñafiel, M., Flores, D. (2023). Competitive adsorption of drugs from a multi-component mixture on sugarcane bagasse. Water, 15(11), DOI: 10.3390/w15112127.

[9] Babalola, B., Adegoke, O., Akintayo, C., Lawal, O., Abimbade, S., Oseghe, E., Ayanda, O. (2020). Adsorption and desorption studies of *Delonix regia* pods and leaves: removal and recovery of Ni(II) and Cu(II) ions from aqueous solution. *Drinking Water Engineering Science, 13*(4), 15-27. DOI: 10.5194/dwes-13-15-2020

[10] Noroozi, B., Sorial, G.A. (2013). Applicable models for multi-component adsorption of dyes: A review. *Journal of Environmental Sciences*, 25(3), 419-429. DOI: 10.1016/S1001-0742(12)60194-6

[11] Zahmatkesh, S., Bokhari, A., Karimian, M., AbdulZahra, M., Sillanpää, M., Pancha, H., Rezakhani, Y. (2022). A comprehensive review of various approaches for treatment of tertiary wastewater with emerging contaminants: what do we know? *Environmental Monitoring and Assessment, 6*(10), 1-15. DOI: 10.1007/s10661-022-10503-z

[12] Etim, J., Umoren, A., Eduok, M. (2016). Coconut coir dust as a low-cost adsorbent for the removal of cationic dye from aqueous solution. *Journal of Saudi Chemical Society, 20*, S67-S76. DOI: 10.1016/j.jscs.2012.09.014

[13] Lach, J. (2019). Adsorption of Chloramphenicol on Commercial and Modified Activated Carbons. *Water, 11*(41), 1-17. DOI: 10.3390/w11061141

[14] Nomngongo, N., Chaba, M. (2019). Effective adsorptive removal of amoxicillin from aqueous solutions using zinc oxide-coated carbon nanofiber composite. *Emerging Contaminants, 5*(8), 143-149. DOI: 10.1016/j.emcon.2019.04.001

[15] Terreni, M., Taccani, M., Pregnolato, M. (2021). New Antibiotics for Multidrug-Resistant Bacterial Strains: Latest Research Developments and Future Perspectives. *Molecules, 26*(9), 2671. DOI: 10.3390/molecules26092671

[16] Ghiorghita, C.A., Dinu, M.V., Lazar, M.M., Dragan, E.S. (2022). Polysaccharide-based composite hydrogels as sustainable materials for removal of pollutants from wastewater. *Molecules*, *27*(23), 8574. DOI: 10.3390/molecules27238574

[17] Abulude, F.O., Adejayan, A.W. (2017). Nutritional values of flamboyant (*Delonix regia*) seeds obtained in Akure, Nigeria. *PeerJ Preprints*. https://doi.org/10.7287/peerj.preprints.2764v1

[18] Dada, E.O., Ojo, I.A., Alade, A.O., Afolabi, T.J., Jimoh, M.O., Dauda, M.O. (2020). Biosorption of Bromo-based Dyes from Wastewater Using Low-Cost Adsorbents: A Review. *Journal of Scientific Research and Reports, 26*(8), 34-56. DOI: 10.9734/jsrr/2020/v26i830294

[19] Mondal, I.H., Haque, O. (2016). Synthesis and Characterization of Cellulose-based Eco-Friendly Hydrogels. *Rajshahi University Journal of Science and Engineering, 44*(1), 45-53. DOI: 10.3329/rujse.v44i0.30386

Copyright © 2027, ISSN: 3032-7059

[20] Zhu, W., Zhang, Y., Wang, P., Yang, Z., Yasin, A., Zhang, L. (2019). Preparation and applications of salt-resistant superabsorbent poly (acrylic acid-acrylamide/fly ash) composite. *Materials*, *12*(4), 596. DOI: 10.3390/ma12040596

[21] Al-Niaeem, H., Abdulwahid, A., Hanoosh, W. (2021). Removal of Carcinogenic Dyes Congo red (CR) and Bismarck brown Y (BBY) by Adsorption onto Reusable Hydrogels Derived from Acrylamide. *3rd International Virtual Conference of Chemistry Journal of Physics, 2*(5), 1-29. DOI: 10.1088/1742-6596/2063/1/012011

[22] Yaoning, C., Linshenzhang, L., Yuanping, L., Yihuan, L., Yanrong, C., Hui, L., and Yuqing, L. (2021). Preparation of a double-network hydrogel based on wastepaper and its application in the treatment of wastewater containing copper(II) and methylene blue. *Royal Society of Chemistry Advances, 11*(1), 18131-18143. DOI: 10.1039/D1RA02321G

[23] Tan, Y., Yalini, M., Mah, C., Teo, T., Deen, G. (2022). Synthesis, Swelling Characteristics, and Dye Adsorption Mechanism of a New Stimuli-Responsive Cationic Hydrogel. *European Journal of Advanced Chemistry Research, 3*(1), 12-24. 10.24018/ejchem.2022.3.1.86

[24] Hou, Y., Deng, B., Wang, S., Ma, Y., Long, X., Wang, F., Qin, C., Liang, C., Yao, S. (2023). High-Strength, High-Water-Retention Hemicellulose-Based Hydrogel and Its Application in Urea Slow Release. *International Journal of Molecular Sciences*, 24(11), 9208. DOI: 10.3390/ijms24119208

[25] Putri, R.W., Rahmatullah, R., Len, K.Y., Haryani, N., Susanti, S., Haryati, S., Aliyah, S.T. (2023). Briquette of Rice Husk and Bagasse Mixture with Variation on Adhesive Type and Mass Ratio of Raw Materials. *Chemical Engineering Transactions*, *10(6)*, 277-282. DOI: 10.3303/CET23106047

[26] Dada, E.O., Ojo, I.A., Alade, A.O., Afolabi, T.J., Amuda, O.S., Jameel, A.T. (2020). Biosorption of Bromophenol Blue from Aqueous Solution Using Flamboyant (*Delonix regia*) Pod. *Chemical Science International Journal, 29*(5), 32-50. DOI: 10.9734/CSJI/2020/v29i530179

[27] Ding, D., Yang, S., Qian, X., Chen, L., Cai, T. (2020). Nitrogen-doping positively, whilst sulfur-doping negatively affects the catalytic activity of biochar for the degradation of organic contaminants. *Applied Catalysis B: Environmental*, *26(3)*, 83-98. DOI: 10.1016/j.apcatb.2019.118348

[28] Idan, I.J., Abdullah, L.C., Choong, T.S., Jamil, S.N. (2018). Equilibrium, kinetic, and thermodynamic adsorption studies of acid dyes on adsorbent developed from kenaf core fiber. *Adsorption Science and Technology, 36* (2), 694-712. DOI: 10.1177/0263617417715532

[29] Mecha, C.A., Ouma, K.S., Omayio, B.O. (2024). Insight into the Bouguer-Beer-Lambert Law: A review. *Sustainable Chemical Engineering, 5*(2), 568-574. DOI: 10.37256/sce.5220245325

[30] Seyed, M.M., Khalilollah, M. (2019). Removing Methylene Blue from Aqueous Solutions Using Rice Husk Silica Adsorbent. *Polish Journal of Environmental Studies, 28*(4), 2281-2287. DOI: 10.15244/pjoes/91044

[31] Azad, A.K., Taweekun, J., Saidur, R., Abubakar, M.S., Radenahmad, N., Afroze, S. Reza, M.S. (2020). Preparation of activated carbon from biomass and its applications in water and gas purification: a review. *Arab Journal of Basic and Applied Sciences, 27*(1), 208-238. DOI: 10.1080/25765299.2020.1766799

[32] Fisli, A., Safitr, D., Sari, H., Deswita, D., Nurhasni, R. (2021). Isotherm, Kinetic and Thermodynamic Adsorption Studies of Dye Onto Fe3O4 Waste Paper Activated Carbon Composites. *Journal Technology (Sciences and Engineering), 83*(1), 45-55. DOI: 10.11113/jurnalteknologi.v83.14991

[33] Ezzati, R. (2020). Derivation of Pseudo-First-Order, Pseudo-Second-Order and Modified Pseudo-First-Order rate equations from Langmuir and Freundlich isotherms for adsorption. *Chemical Engineering Journal, 30*(8), 1-13. DOI: 10.1016/j.cej.2019.123705

[34] Murphy, O.P., Vashishtha, M., Palanisamy, P., Kumar, K.V. (2023). A review of the adsorption isotherms and design calculations for the optimization of adsorbent mass and contact time. *ACS Omega*, *8*(20), 407-430. DOI: 10.1021/acsomega.2c08155

[35] Inyinbor, A.A., Adekola, F.A., Olatunji, G.A. (2015). Adsorption of Rhodamine B Dye from Aqueous Solution on Irvingia gabonensis Biomass: Kinetic and Thermodynamic Studies.*South African Journal of Chemistry, 6*(8), 115-125. DOI: 10.17159/0379-4350/2015/v68a17

[36] Popoola, L.T. (2020). Tetracycline and sulfamethoxazole adsorption onto nanomagnetic walnut shell-rice husk: isotherm, kinetic, mass transfer diffusion, and thermodynamic studies. *International Journal of Environmental Analytical Chemistry, 10*(9), 1021-1043. DOI: 10.1080/03067319.2019.1646739

Copyright © 2027, ISSN: 3032-7059

[37] Asare, E., Dartey, E., Sarpong, K., Effah-Yeboah, E., Amis-Sah, P., Tagoe, S., Balali, G. (2021). Adsorption Isotherm, Kinetic and Thermodynamic Modeling of Bacillus subtilis Mediated Adsorption of Arsenic in Groundwaters of Selected Gold Mining Communities in the Wassa West Municipality of the Western Region of Ghana. *American Journal of Analytical Chemistry, 12*(2), 121-161. DOI: 10.4236/ajac.2021.125010

[38] Ewis, D., Ba-Abbad, M.M., Benamor, A., Mahmud, N., Nasser, M., El-Naas, M., Mohammad, A.W. (2022). Adsorption of 4-nitrophenol onto iron oxide bentonite nanocomposite process optimization, kinetics, isotherms and mechanism. *International Journal of Environmental Research*, *16*(2), 1-23. DOI: 10.1007/s41742-022-00402-z

[39] Mogharbel, R., Alkhamis, K., Felaly, R., El-Desouky, M., El-Bindary, A., El-Metwaly, N., El-Bindary, M. (2024). Superior adsorption and removal of industrial dye from aqueous solution via magnetic silver metal-organic framework nanocomposite. *Environmental Technology*, 45(13), 58-74. DOI: 10.1080/09593330.2023.2178331

[40] Dehghani, M., Tajik, S., Panahi, A., Khezri, M., Zarei, A., Heidarinejad, Z., Yousefi, M. (2018). Adsorptive removal of noxious cadmium from aqueous solutions using polyurea-formaldehyde: A novel polymer adsorbent. *Methods, 5*(1), 1148-1155. DOI: 10.1016/j.mex.2018.09.010

[41] Wahab, M., Zahoor, M., Salman, S.M. (2019). A novel approach to remove ofloxacin antibiotic from industrial effluent using magnetic carbon nanocomposite prepared from sawdust of Dalbergia sissoo by batch and membrane hybrid technology. *Desalination and Water Treatment, 16(5)*, 83-96. DOI: 10.5004/dwt.2019.24573

[42] Amole, A.R., Araromi, D.O., Alade, A.O., Afolabi, T.J., Adeyi, V.A. (2021). Biosorptive removal of nitrophenol from aqueous solution using $ZnCl_2$-modified groundnut shell: optimization, equilibrium, kinetic, and thermodynamic studies. *International Journal of Environmental Science and Technology, 18*(10), 59-76. DOI: 10.1007/s13762-020-02939-y

[43] Qili, H., Zhenya, Z. (2019). Application of Dubinin-Radushkevich isotherm model at the solid/solution interface: A theoretical analysis. *Journal of Molecular Liquids, 27*(1), 646-648. DOI: 10.1016/j.molliq.2019.01.005

[44] Abiodun, O.O., Oluwaseun, O., Oladayo, O. K., Abayomi, O., George, A. A., Opatola, E., Omotayo, I. A. (2024). Remediation of heavy metals using biomass-based adsorbents: adsorption kinetic and isotherm models. *Clean Technologies*, *5*(3), 934-960. DOI: 10.3390/cleantechnol5030047

[45] Nandiyanto, A., Nugraha, W., Yustia, I., Ragadhita, R., Fiandini, M., Meirinawati, H., Wulan, D. (2024). Isotherm and kinetic adsorption of rice husk particles as a model adsorbent for solving issues in the sustainable gold mining environment from mercury leaching. *Journal of the Mining Institute,* 26(5), 104-120. DOI: 10.31897/PMI.2024.19

[46] Karim, S. S., Farrukh, S., Fan, X., Yu, Z. (2025). Adsorption in Multi-layer Composite Membranes for Gas Separation Applications. In Multi-Layer Composite Membranes for Gas Separation (Springer, Cham, Vol. 102, pp. 103–158.

[47] Sharma, N., Tiwari, A. (2014). Nano iron oxide loaded Poly (Acrylonitrile-co-Acrylic acid) hydrogel applied as Novel adsorbent for Effective removal of Toxic Cd^{2+} ions using Fixed-bed Micro column technology. *Research Journal of Chemical Sciences*, 4(9), 88-100.

[48] Díaz-Montes, E. (2022). Polysaccharides: Sources, characteristics, properties, and their application in biodegradable films. *Polysaccharides*, *3*(3), 480-501. DOI: 10.3390/polysaccharides3030029

[49] Lan, Y.T., Cheng, Q.P., Xu, J., Lin, S.H., Lin, J.M., Hsu, S.H. (2022). Gelation and the self-healing behavior of the chitosan-catechol hydrogel. *Polymers*, *14*(21), 46-54. DOI: 10.3390/polym14214614

[50] Godiya, C.B., Cheng, X., Li, D., Chen, Z., Lu, X. (2019). Carboxymethyl cellulose/polyacrylamide composite hydrogel for cascaded treatment/reuse of heavy metal ions in wastewater. *Journal of hazardous materials*, *36(4),* 28-38. DOI: 10.1016/j.jhazmat.2018.09.076

[51] Eden, W.T., Rumambarsari, C.O. (2020). Proximate analysis of soybean and red bean cookies according to the Indonesian National Standard. In Journal of Physics: *Conference Series* 15 (2), 1-6. DOI: 10.1088/1742-6596/1567/2/022033

[52] Adekanye, T., Dada, O., Kolapo, J. (2022). Pyrolysis of maize cob at different temperatures for biochar production: Proximate, ultimate and spectroscopic characterisation. *Research in Agricultural Engineering, 68*(1), 27-34. DOI: 10.17221/106/2020-RAE

[53] Iwar, R.T., Utsev, J.T., Ifyalem, K.J. (2020). Adsorption of Methylene Blue from Aqueous Solution onto *Delonix regia* Pod Activated Carbon: Batch Equilibrium Isotherm, Kinetic and Thermodynamic Studies. *Journal of Materials and Environmental Science, 11*(7), 1058-1078.

Copyright © 2027, ISSN: 3032-7059

[54] Oluwasina, O., James, O.A., Lukman, B., Olayinka, O., Olusegun, O. (2020). *Delonix regia* seeds and pods: characterization and its potential as a feedstock for thermochemical conversion. *Journal of Applied Chemistry*, *13(3)*, 39-49. DOI: 10.9790/5736-1303013949

[55] Krotz, L., Giazzi, G. (2017). Elemental analysis: CHNS/O characterization of carbon black compliance with ASTM D5373 method (Application Note No. 42238). Retrieved from Thermo Fisher Scientific website: pragolab.cz

[56] Yahya, M D., Obayomi, K.S., Abdulkadir, M.B., Iyaka, Y.A., Olugbenga, A.G. (2020). Characterization of cobalt ferrite-supported activated carbon for removal of chromium and lead ions from tannery wastewater via adsorption equilibrium. *Water Science and Engineering,* *13*(3), 202-213. 10.1016/j.wse.2020.09.007

[57] Adedipe, D.T., Bayode, A.A., Ore, O.T. (2025). Progress in the application of graphene-based nanomaterials for gas adsorption and mitigation of air pollution. *Royal Society of Chemistry Advances, 15*(38), 32-59. DOI: 10.1039/D5RA04635A

[58] Quillo, G.L., Bhonsale, S., Collas, A., Xiouras, C., Van Impe, J.F. (2023). Iterative model-based optimal experimental design for mixture-process variable models to predict solubility. *Chemical Engineering Research and Design*, *18(9)*, 768-780. DOI: 10.1016/j.cherd.2022.12.006

[59] Sadergaski, L.R., Toney, G.K., Delmau, L.H., Myhre, K.G. (2021). Chemometrics and experimental design for the quantification of nitrate salts in nitric acid: Near-infrared spectroscopy absorption analysis. *Applied Spectroscopy*, *75*(9), 1155-1167. DOI: 10.1177/0003702820987281

[60] Sazali, N., Harun, Z., Sazali, N. (2020). A review on batch and column adsorption of various adsorbents towards the removal of heavy metals. *Journal of Advanced Research in Fluid Mechanics and Thermal Sciences*, *67*(2), 66-88.

[61] Mohamed, N.B., Ngadi, N., Yahya, N. Y., Mohamed, M.H., Bakar, A.A., Ali, N. (2025). Optimization Study of Ammonium Adsorption from Aqueous Solution on Carbon Black Modified with Sodium Dodecylbenzene Sulfonate: Kinetic, Isotherms, and Thermodynamics. *Arabian Journal for Science and Engineering*, 1-22. DOI: 10.1007/s13369-024-09914-6

[62] Mikolajczyk, A.P., Fortela, D.L, Berry, J.C., Chirdon, W.M., Hernandez, R.A., Gang, D.D., Zappi, M.E. (2024). Evaluating the suitability of linear and nonlinear regression approaches for the Langmuir adsorption model as applied toward biomass-based adsorbents: Testing residuals and assessing model validity. *Langmuir*, *40*(39), 428-442. DOI: 10.1021/acs.langmuir.4c01786

[63] Hani, Z., Damla, O., Nezahat, K., Erol, P., Ahmetli, G., Marti, M. E. (2020). Separation of formic acid and acetic acid from aqueous solutions using sugar beet processing fly ash: characterization, kinetics, isotherms and thermodynamics. *Desalination and Water Treatment*, 20(2), 283-294. DOI: 10.5004/dwt.2020.26142

[64] Mansoori, S., Reza, Z., Mohammad, H., Mohammad, M., Abolfazl, J., Sadegh, S., Akbar, E. (2022). HSS anion reduction combined with the analytical test of aqueous MDEA in South Pars gas complex. *Natural Gas Industry B*, *9*(3), 318-324. DOI: 10.1016/j.ngib.2022.06.004

[65] Acharya, A., Jeppu, G., Raju Girish, C., Prabhu, B. (2023). Development of a multicomponent adsorption isotherm equation and its validation by modeling. *Langmuir*, *39*(49), 862-878. DOI: 10.1021/acs.langmuir.3c02496

[66] Chen, R., Yang, S., Liu, B., Liao, Y. (2023). Eco-Friendly Semi-Interpenetrating Polymer Network Hydrogels of Sodium Carboxymethyl Cellulose/Gelatin for Methylene Blue Removal. *Materials*, 16(33), 1-17. DOI: 10.3390/ma16093385

[67] Rajalekshmi, G.A., Mrithaa, T.S.A., Viji-Chandran, S.A., Pandimadevi, M.A. (2016). Preparation and characterisation of activated carbon from *Delonix regia* seeds for the removal of methylene blue dye. *Journal of Industrial Pollution Control*, 32(2), 572-579.

[68] Chang, J., Shen, Z., Hu, X., Schulman, E., Cui, C., Guo, Q., Tian, H. (2020). Adsorption of tetracycline by shrimp shell waste from aqueous solutions: adsorption isotherm, kinetic modeling, and mechanism. *ACS Omega*, 5(7), 67-77. DOI: 10.1021/acsomega.9b03781

[69] Tang, Y., Jia, W., Bao, M., Qiu, S., Pi, Y., Liu, C., Zhao, J. (2023). Pick-up of fluoroquinolones from the aqueous phase via magnetically propelled microrobots: kinetic, thermodynamics, and site energy distribution analysis. *Frontiers in Marine Science*, 10(11), 116-129. DOI: 10.3389/fmars.2023.1169883

Copyright © 2027, ISSN: 3032-7059

[70] Lach, J. (2024). Kinetics, statics, and thermodynamics of ampicillin adsorption on microporous carbon sorbents. *Desalination and Water Treatment*, 31(7), 1-12. DOI: 10.1016/j.dwt.2024.100144

[71] Rani, K., Singh, J., Jangra, A., Kumar, J., Kumar, P., Kumar, S., Kumar, R. (2023). Kinetic and isotherm investigations on the improved adsorption of the antibiotic moxifloxacin from aqueous solution utilizing agar-coated magnetite nanoparticles. *Biointerface Research in Applied Chemistry*, 1(3), 48-60. DOI: 10.33263/BRIAC135.480

[72] Davoodi, S., Dahrazma, B., Goudarzi, N., Gorji, H. (2019). Adsorptive removal of azithromycin from aqueous solutions using raw and saponin-modified nano diatomite. *Water Science and Technology, 80*(5), 939-949. DOI: 10.2166/wst.2019.337

[73] Edet, U.A., Ifelebuegu, A.O. (2020). Kinetic, isotherms, and thermodynamic modeling of the adsorption of phosphates from model wastewater using recycled brick waste. *Processes*, 8(6), 1-15. DOI: 10.3390/pr8060665

[74] Yeo, J., Khaerudini, D., Soetaredjo, F., Waworuntu, G., Ismadji, S., Sunarso, J., Liu, S. (2023). Isotherm data for adsorption of amoxicillin, ampicillin, and doripenem onto bentonite. *Data in Brief*, 4(8), 1091-1098. DOI: 10.1016/j.dib.2023.109159

[75] Khumalo, S.M., Bakare, B.F., Rathilal, S. (2024). Single and multicomponent adsorption of amoxicillin, ciprofloxacin, and sulfamethoxazole on chitosan-carbon nanotube hydrogel beads from aqueous solutions: Kinetic, isotherms, and thermodynamic parameters. *Journal of Hazardous Materials Advances*, *13*(2), 1004-1016. DOI: 10.1016/j.hazadv.2024.100404

[76] Mustapha, S.I., Adewoye, L.T., Aderibigbe, F.A., Alhaji, M.H., Adekola, M.I., Tijani, I.A. (2019). Removal of Lead and Chromium from Aqueous Solution onto Flamboyant (*Delonix regia*) Pod Activated Carbon. *Nigerian Journal of Technological Development, 14*(2), 56-66. DOI: 10.4314/njtd.v14i2.4

[77] Somyanonthanakun, W., Ahmed, R., Krongtong, V., Thongmee, S. (2023). Studies on the adsorption of Pb (II) from aqueous solutions using sugarcane bagasse-based modified activated carbon with nitric acid: kinetic, isotherm and desorption. *Chemical Physics Impact*, 6, 1-13 DOI: 10.1016/j.chphi.2023.100181

[78] Sharifmand, M., Sepehr, E., Rasouli-Sadaghiani, M., Asri-Rezaei, S., Rengel, Z. (2024). Antibiotic pollutants in agricultural soil: Kinetics, sorption, and thermodynamics of ciprofloxacin. *Heliyon*, *10*(18). DOI: 10.1016/j.heliyon.2024.e37035

[79] Ojediran, J.O., Dada, A.O., Aniyi, S.O., David, R.O., Adewumi, A.D. (2021). Mechanism and isotherm modeling of effective adsorption of malachite green as endocrine disruptive dye using Acid Functionalized Maize Cob. *Scientific Reports*, 11(1), 2149-2163. DOI: 10.1038/s41598-021-00993-1

Copyright © 2027, ISSN: 3032-7059